



HORIZON 2020
THEME SC5-2017



European Climate Prediction system

(Grant Agreement 776613)

European Climate Prediction system (EUCP)

Deliverable D4.6

Outlook of future hazards for the outermost regions

Deliverable Title	<i>Outlook of future hazards for the outermost regions</i>	
Brief Description	<i>This deliverable provides an outlook of trends in future flood hazard and impacts for two outermost regions in the Caribbean and of La Reunion (Indian Ocean) building upon the climate simulations made available by WP3.</i>	
WP number	4	
Lead Beneficiary	<i>Deltares</i>	
Contributors	<i>Panos Athanasiou, Deltares</i> <i>Tycho Bovenschen, Deltares</i> <i>Dirk Eilander, Deltares</i> <i>Sanne Muis, Deltares</i> <i>Jelmer Veenstra, Deltares</i> <i>Hylke de Vries, KNMI</i> <i>Albrecht Weerts, Deltares</i> <i>Frederiek Sperna Weiland, Deltares</i>	
Creation Date	<i>17-03-2022</i>	
Version Number	<i>1.0</i>	
Version Date	<i>18-05-2022</i>	
Deliverable Due Date	<i>31/03/2022</i>	
Actual Delivery Date	<i>31/05/2022</i>	
Nature of the Deliverable	<input checked="" type="checkbox"/> X <input type="checkbox"/> <input type="checkbox"/> <input type="checkbox"/>	<i>R – Report</i> <i>P – Prototype</i> <i>D - Demonstrator</i> <i>O – Other</i>
Dissemination Level/ Audience	<input checked="" type="checkbox"/> PU <input type="checkbox"/> <input type="checkbox"/> <input type="checkbox"/>	<i>PU – Public</i> <i>PP - Restricted to other programme participants, including the Commission services</i> <i>RE - Restricted to a group specified by the consortium, including the Commission services</i> <i>CO - Confidential, only for members of the consortium, including the Commission services</i>

Version	Date	Modified by	Comments
0.1	9-4-2022	Frederiek Sperna Weiland	First version
0.2	15-4-2022	Ap van Dongeren	WP4 internal review
0.3	21-4-2022	Frederiek Sperna Weiland	Report revision
0.4	17-5-2022	Albrecht Weerts	Update case-study La Reunion
0.5	17-5-2022	Carol McSweeney	Project review
1.0	18-5-2022	Frederiek Sperna Weiland	Final version

Table of contents

1	Executive summary	5
	1.2 Summary Caribbean case	5
	1.2 Summary La Reunion case	6
2	Project objectives	8
3	Detailed report	8
	3.1.1 Caribbean Islands - Brief introduction to the case-study	10
	3.1.2 Approach	11
	3.1.3 Models	13
	3.1.4 Data – input and static data used in the modelling chain	20
	3.1.3 Results	21
	3.1.3.1 <i>METEO</i>	21
	3.1.3.2 <i>GTSM</i>	25
	3.1.3.3 <i>SFINCS</i>	27
	3.1.3.4 <i>FIAT</i>	34
	3.1.4 Discussion and lessons learned	38
	3.1.5 Assumptions and simplifications made to complete data requirements	39
	3.2.1 LaReunion - Brief introduction to the case-study	40
	3.2.2 Data and Methods	41
	3.2.3 Results	45
	3.2.4 Discussion and lessons learned	46
	References	47

1 Executive summary

This report summarizes two future climate impact assessments for the EU outermost regions focussing on flood hazard and impacts. The work builds upon European convection-permitting (CP) regional climate simulations that were prepared by the climate modellers from WP3. Within the second year the EU requested the EUCP project consortium to extend the work to the European outermost regions. WP3 partners have implemented model simulations for the Caribbean domain, the island of La Reunion and The Canary Islands and Madeira. Based on these simulations two future hazard outlooks have been conducted in WP4:

- The assessment of future changes in tropical cyclone strength and impacts over the Caribbean Islands of Martinique, Sint-Martin and the Dominican Republic;
- The assessment of future changes in low and high flows for La Reunion.

This report provides a summary of these assessments. Next to the future outlooks, this report also discusses the difficulties experienced and the assumptions that had to be made for the cyclone analysis.

1.2 Summary Caribbean case

To assess the future changes in flood impacts caused by cyclones over the Caribbean Islands we implemented a modelling chain that includes meteorology, hydrodynamics of surge and waves, flooding and damages (Figure 1.1).

The climate projections that drive the modelling chain are obtained from the Convection-Permitting Regional Climate Modelling (CP-RCM) system HARMONIE-Climate (HCLIM; Belusic et al., 2019). The Dutch Meteorological Institute (KNMI) ran the model following a pseudo-global warming (PGW) approach. In this approach, a re-analysis dataset is used for the HCLIM historical boundary conditions (ERA5). For the future period seasonal varying delta-changes have been applied to these re-analysis boundary conditions to obtain 'futurized' conditions of the current climate events corresponding to a 2-degrees warmer world. The HCLIM simulations were run for the historic and future cyclone season (June-Oct).

Figure 1.1 depicts the full modelling chain. The wind speed and air pressure from the HCLIM simulations are input for the hydrodynamic Global Tide and Storm Surge model (GTSM; Muis et al., 2020) together with ERA5 wave data. Sea level rise was added to the GTSM results based on global IPCC estimates. The river discharges and effective precipitation calculated with the hydrological wflow_sbm model and the GTSM results are input into the Super-Fast Inundation of CoastS overland flooding model (SFINCS; Leijnse et al., 2020) to produce flood maps for the current and future climate. These flood maps were input into the flood impact damage module (FIAT; Slager et al., 2016) that calculates the economic damage and affected population.

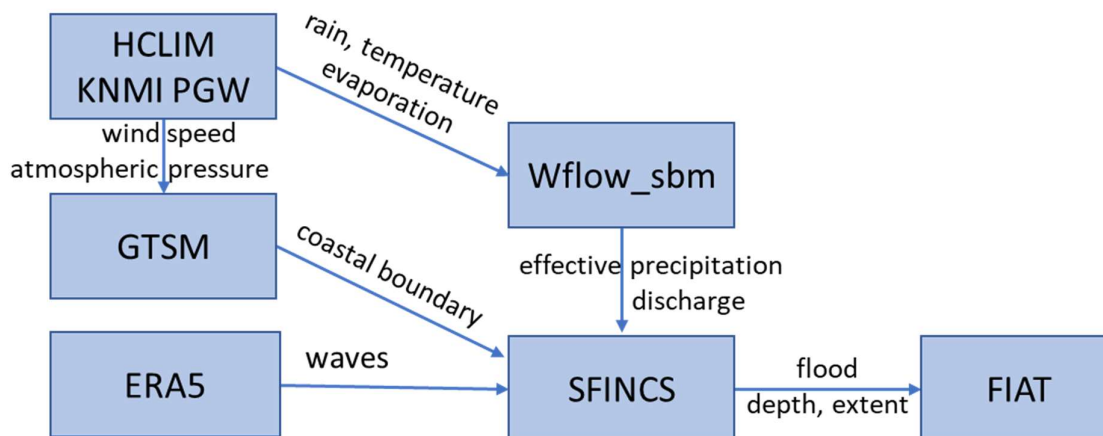


Figure 1.1: overview of the modelling chain employed to assess flood impacts for the current and future climate

The analysis focused on the year 2017 which was characterized by an extremely active tropical cyclone season with six major cyclones (cat 3-5).

The original plan for the analysis and presentation of future changes was a storyline approach (Shepherd et al., 2018; Sillmann et al., 2021). With the storyline approach the behaviour of historic extreme weather events is transferred to future warming conditions. One of the main difficulties of this storyline approach for tropical cyclones is their large inter-annual variability and their non-linear dynamics. The random spatial shifts in cyclone track between the evaluation (i.e., the current climate) and future PGW experiment, determine whether the impact along the historical track will locally increase or decrease in the future. For all storms analysed changes in position were obtained. This resulted in changes in flood impacts on the islands that were not primarily caused by climate change, but by changes in the cyclone track. Only for Tropical Cyclone Irma at Sint-Martin we found increases in flood impacts for the future climate simulations compared to the evaluations run. However, during the cyclone season of 2017 the observed storms were very close together. The future heavy precipitation is rather likely caused by the intensification of storm Jose than by the intensification of Irma. The use of a large climate model ensembles (van Oldenborgh et al., 2017; Van der Wiel et al., 2019), synthetic event generation like TCWise (Nederhoff et al., 2021; Bloemendaal et al., 2020; Lin et al., 2012) or machine learning approaches could be an alternative approach to analyse the climate change impact. Thus, the multi-model CP-RCM dataset from EUCP WP3 would be a valuable instrument for a follow-up of this case-study.

1.2 Summary La Reunion case

The second climate change assessment for the outermost regions focusses on potential future changes in flood and drought extremes for La Reunion. La Reunion is located in the Indian Ocean approximately 550 km east of the island of Madagascar. The island is regularly threatened by tropical cyclones. For this case CP-RCM simulations were provided by CNRM.

A distributed hydrological model (wflow_sbm) was implemented for the Island at a spatial resolution of 200 metres. The model simulated flows were compared against available discharge observations

from hydrobanque (<https://hubeau.eaufrance.fr>). This reference hydrological model run was based on a meteorological dataset of interpolated precipitation fields obtained from MeteoFrance (1979-2019) at 1km² resolution. The same dataset was used to bias-correct the CP-RCM climate simulations that showed relatively large biases from the local observations. Compared to the Caribbean Islands there is a relatively large amount of precipitation and discharge observations available for La Reunion which could be used to improve the assessment.

For the climate assessment the model was forced with both historical data and bias-corrected future CP-RCM simulations provided by CNRM. Based on the current and future climate simulations we conclude that annual extremes could increase even up to 30% by 2100 under a high emission scenario, and will possibly cause more devastating flooding across La Reunion. The simulations also show that the discharge regime will become more variable. According to these runs the annual mean discharge will only decrease slightly (~2%).

2 Project objectives

The deliverable has contributed to the following EUCP objectives:

No.	Objective	Yes	No
1	Develop an ensembles climate prediction system based on high-resolution climate models for the European region for the near-term (~1-40 years)	X	
2	Use the climate prediction system to produce consistent, authoritative and actionable climate information	X	
3	Demonstrate the value of this climate prediction system through high impact extreme weather events in the near past and near future	X	
4	Develop, and publish, methodologies, good practice and guidance for producing and using EUCP's authoritative climate predictions for 1-40 year timescales	X	

3 Detailed report

Besides the European continent, the European Union comprises nine outermost regions. Ideally, developments in EU projects enable future climate hazard outlooks for these outermost regions as well and within the second year of EUCP the European Commission specifically requested to extend the work to the outermost regions.

This report summarizes two case-studies conducted for these outermost regions as part of the WP4 work. The aim of the case-studies was to demonstrate the application of simulations at convection-permitting scales to assess future hydro-meteorological risks (e.g., for tropical cyclones, sea level rise, coastal, pluvial and river flood). Especially here, the convection permitting simulations were expected to provide improved information.

With these case-studies we demonstrate the current value of the climate prediction system and evaluate what we can do with the current climate model data for the outermost regions and the specific hazards experienced. In addition, we have identified a number of improvements in climate simulation availability and approaches to best employ those that would be of great benefit for similar assessments in the future. These examples test the application of individual ensemble members from the Convection Permitting Regional Climate Model (CP-RCM) simulations – further work is recommended to develop a multi-model approach making use of the multiple CPM simulations generated by WP3 (See EUCP deliverable D3.5 for details of CPM experimental design and analysis of the simulations).

We present two applications:

- Future changes in cyclone risk for the Caribbean islands Martinique, Sint-Martin and the Dominican Republic using the CP-RCM Harmonie-CLIM simulations from KNMI;
- Future changes in (flash) flood occurrence and low flows for La Reunion using the CP-RCM AROME simulations from CNRM.

3.1 Assessment of future changes in tropical cyclone impact over the Caribbean

3.1.1 Caribbean Islands - Brief introduction to the case-study

In this case-study we assess the value of high-resolution CP-RCM climate data for estimating potential changes in cyclones occurrence for the Caribbean Islands Martinique, Saint-Martin and the Dominican Republic. The first two are outermost EU regions, the latter not. The Dominican Republic was included because it is one of the Caribbean Islands most prone to cyclones. It was also severely impacted by the cyclones of 2017, the year of interest for the current study.

The Caribbean islands are located in an area prone to cyclones, which occurs from June to November. The year-to-year variability is large, with some seasons having few major cyclones and others season having more than four. The strongest cyclones in the Caribbean typically originate near the Cabo Verde islands at the western coast of Africa, gain strength as they pass westward over the Atlantic Ocean, and rapidly weaken when they make landfall or propagate into cooler waters. Tropical cyclones are associated with strong winds and high aggregated rainfall. They can induce extremely high water levels at the coast due to the generation of a storm surge and waves. This can cause extensive (compound) flooding. Besides causing Sea Level Rise (SLR), climate change may affect cyclone frequency and severity. Here we will investigate whether in the future cyclone impacts will change. For instance, increasing sea-surface temperature (SST) will potentially provide more energy to tropical cyclones through increased evaporation and latent-heat release, thereby making them larger, wetter (Clausius-Clapeyron) and more intense (see e.g., Oldenborgh et al. 2017).

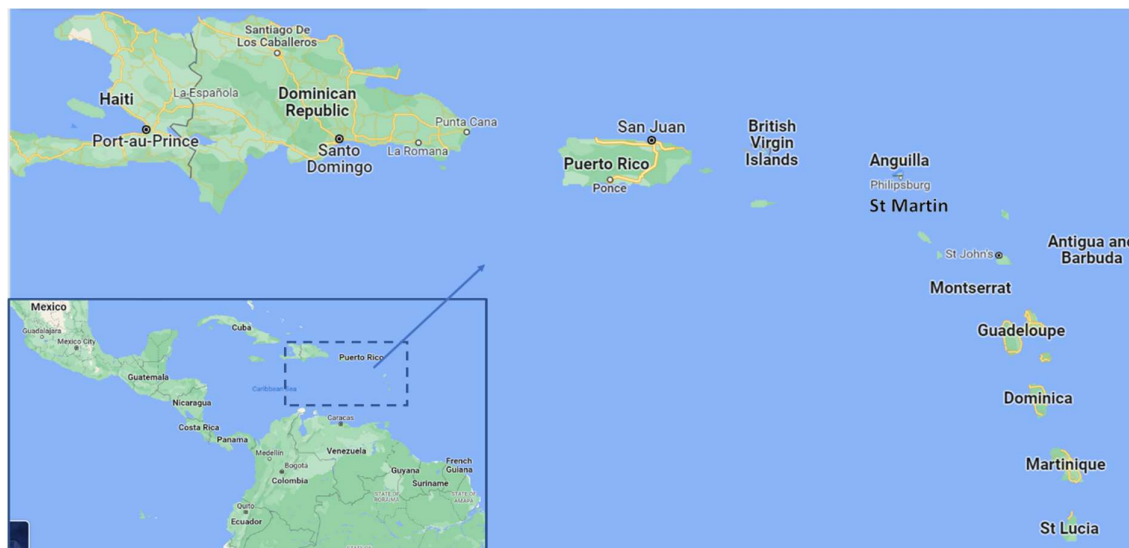


Figure 3.1: Overview map of the Caribbean Islands, including the Dominican Republic, St Martin and Martinique (source: Google Maps).

Any change in cyclone frequency combined with sea-level rise poses a severe risk to the Caribbean islands and its population. Beaches and coastal ecosystems, such as coral reefs, mangroves and seagrass beds, will be impacted. Small island states are particularly vulnerable since the economies and livelihoods of these islands rely on the preservation of the coastal zone with little accommodation

space and few resources to counter the effects. However, the analysis of how the probabilities of extreme events change in future climate is challenging, especially for tropical cyclones. The conventional approach to assess the impacts of climate change of extremes is probabilistic, based on assessing changes in probabilities based on ensembles of climate model simulations.

However, many of the climate models lack the resolution to adequately represent the high intensities of tropical cyclones (Hodges et al., 2017; Roberts et al., 2020; Schenkel & Hart, 2012). Moreover, extreme events are rare by definition and the inter-annual cyclone variability is large. Therefore, the CP-RCM modellers from WP3 adopted a pseudo-global warming (PGW) approach (Schär et al. 1996). In this PGW experiment the boundary information for the regional climate model was taken from ERA5. The CP-RCMs were run for a selection of at least 10 years with historically high TC-activity. In addition to this reference simulation, a second simulation was performed in which a seasonally varying delta-change signal was added, while retaining the same daily variability as in the reference run, i.e. the so called PGW run. Such a PGW method can nicely tap into a storyline approach (Shepherd et al., 2018; Sillmann et al., 2021) where the behaviour of the current climate event is described under future warming conditions. Here we evaluate the applicability of this approach.

3.1.2 Approach

CASE-STUDY AREA

Martinique is part of France (Wikipedia, 2022¹). The Island has a population of ~380.000 people and a land area of 1.128 km². The Island is volcanic, and the terrain is mountainous. The east coast is most susceptible to cyclones, whereas the Northern part receives most rain on an annual basis. The island has several short and torrential rivers.

The Dominican Republic is the second largest nation in the Antilles (48.671 km²) and is located on the same island as Haiti. The Eastern part and its coastal zones, that are of interest in this study, have a rainforest climate and most cyclones make landfall on this side of the Island. The island has a population of more than 10 million people.

Saint-Martin consists of a Dutch (south) and a French (north) part. The northern part is part of France and thus outermost region. The Dutch part is an independent country in the Kingdom of the Netherlands. The island has an area of 87.000 km² with a population of ~75.000 people (of which 33.000 on the French side). Merely the Dutch part of the island was severely struck by cyclone Irma in 2017. This cyclone caused significant damage of about \$3 billion. One third of the buildings were destroyed.

SELECTED cyclones

In 2017, the cyclone season was extremely active (Fig. 3.2). On average the North Atlantic basin sees 3.4 major cyclones (cat 3–5) per season, but in 2017 there were six major cyclones. This was the result of different meteorological conditions, such as above average sea surface temperatures, low levels of difference in winds, an active West African monsoon producing tropical cyclone seedlings, and sufficient moisture levels in the mid to upper troposphere. Especially major cyclones Irma and Maria caused severe damage in the Caribbean region. Both storms underwent rapid intensification. Due to

¹ [wikipedia.org/wiki/Martinique](https://www.wikipedia.org/wiki/Martinique)

the similar tracks of Irma and Maria through the Caribbean, some islands like Sint-Martin were struck twice. The path of cyclone Jose did not cross over Sint-Martin but did cause strong winds and heavy rains on the island. Although the cyclones did not make landfall on Martinique, both Maria and Harvey affected the island. Maria also passed by the east and north coast of the Dominican Republic and caused severe damage here due to heavy rain and high winds.



Figure 3.2. Satellite image taken at 11:15 a.m. EDT on Sep. 7 showing cyclone Katia (left), cyclone Irma (center), and cyclone Jose (right) hovers just north of the island of Hispaniola, with cyclone Katia, left, in the Gulf of Mexico, and cyclone Jose. Source: NOAA.

PSEUDO-GLOBAL WARMING APPROACH

The climate simulations used for this experiment follow a Pseudo-Global Warming approach. When the climate model is run for the historic period the lateral boundary conditions are supplied by re-analysis data, in this case the ERA5 re-analysis dataset (Hersbach et al., 2020) and the climate model provides its best possible representation of the historic weather. For the future climate simulations the temperature fields are perturbed and approximate the response to 2-degrees global warming. For this study KNMI applied seasonal varying Delta-changes to the ERA5 boundary conditions (see EUCP Deliverable 3.5 and De Vries et al. 2022 for more detail). In this way ‘futurized’ versions of the current climate events are obtained. In general, these kind of PGW experiments are ideal for analysis and presentation of climate change projections following a storyline approach (Shepherd et al., 2018; Sillmann et al., 2021). Within this so-called storyline approach the behaviour of the current climate event is described under future warming conditions.

In the end three scenarios were defined: (1) the *evaluation* scenario that represents the current climate, (2) the *PGW* scenarios that represents the ‘futurized’ situation and (3) the *PGW+SLR* scenario where sea level rise is added on top of the PGW conditions. The latter has been added to compare the

influence of Sea Level Rise and changing atmospheric conditions on future flood impacts caused by cyclones.

FLOOD IMPACT MODELLING CHAIN

To assess changes in future tropical cyclone occurrence and impact, the modelling chain in Figure 3.3 has been established. The individual model components will be discussed in more detail in section 3.1.3. In summary the wind pressure from the HCLIM simulations are input for the hydrodynamic Global Tide and Storm Surge model (GTSM; Muis et al., 2020) together with ERA5 wave data. Sea level rise (SLR) is added to the GTSM results based on global IPCC estimates. The river discharges are calculated with the hydrological wflow_sbm model. These discharges, the effective precipitation and the GTSM results are input into the Super-Fast Inundation of CoastS overland flooding model (SFINCS; Leijnse et al., 2020) to produce flood maps for the current and future climate. Finally, the SFINCS flood maps are input into the flood impact damage module (FIAT; Slager et al., 2016) that calculates the economic damage and affected population.

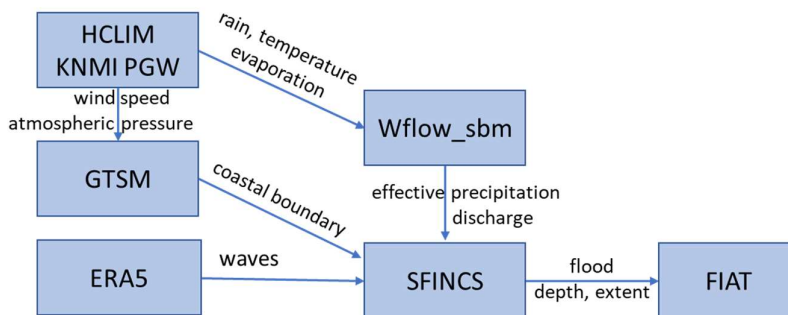


Figure 3.3: overview of the modelling chain employed to assess flood impacts for the current and future climate

3.1.3 Models

DELFT3D FLEXIBLE MESH HYDRODYNAMIC MODEL - GTSM

For the simulation of storm surges and tides, we built a regional hydrodynamic model covering the entire Caribbean domain. The model extents from 8.3 to 26 degrees north and from 85 to 59 degrees east. The model is based on the Delft3D Flexible Mesh software (Kernkamp et al., 2011), and it is a cut-out of the Global Tide and Surge Model (GTSM) version 4.1. The grid has a spatially varying resolution of 1.25km near the coast, while further away from the coast the resolution decreases to 5 km. This results in a high accuracy at relatively low computational costs. The model is run in depth-averaged barotropic mode. The bathymetry is based on General Bathymetric Chart of the Ocean with a 15 arc-seconds resolution (GEBCO, 2020). Tides were modelled by forcing the model with tides from the FES2014 at the boundaries (Lyard et al., 2021). Surges are caused by gradients in the surface pressure of the atmosphere and the transfer of momentum from the wind to the water. We use the relation of Charnock (1955), to estimate the wind stress at the ocean surface. We tested the sensitivity of using different values for the drag coefficient, resulting in minimal differences. Therefore, it was decided to use a drag coefficient of 0.041, consistent with previous work (Muis et al., 2016, 2020). Using the ERA5 reanalysis as forcing, the model was compared against observed sea levels as an initial validation (Figure 3.4). This included about 30 tide gauge stations from the University of Hawaii Sea Level Center dataset (Caldwell et al., 2015), and generally showed a root-mean-squared-error below

10 cm. Maximum surge heights are underestimated compared to observations. This is caused by the underestimation of tropical cyclone intensities in ERA5, also shown by Dullaart et al. (2019). This is mostly due to resolution effects (i.e. 0.25 degree, equivalent to 27-28 km at the equator), which are expected to be much lower in the HCLIM simulations that have a 3~ km resolution and will better capture the high intensities of cyclones (Robert et al., 2020). This is not possible to verify since the HCLIM simulations do not match actual historical events as measured by tide gauge stations.

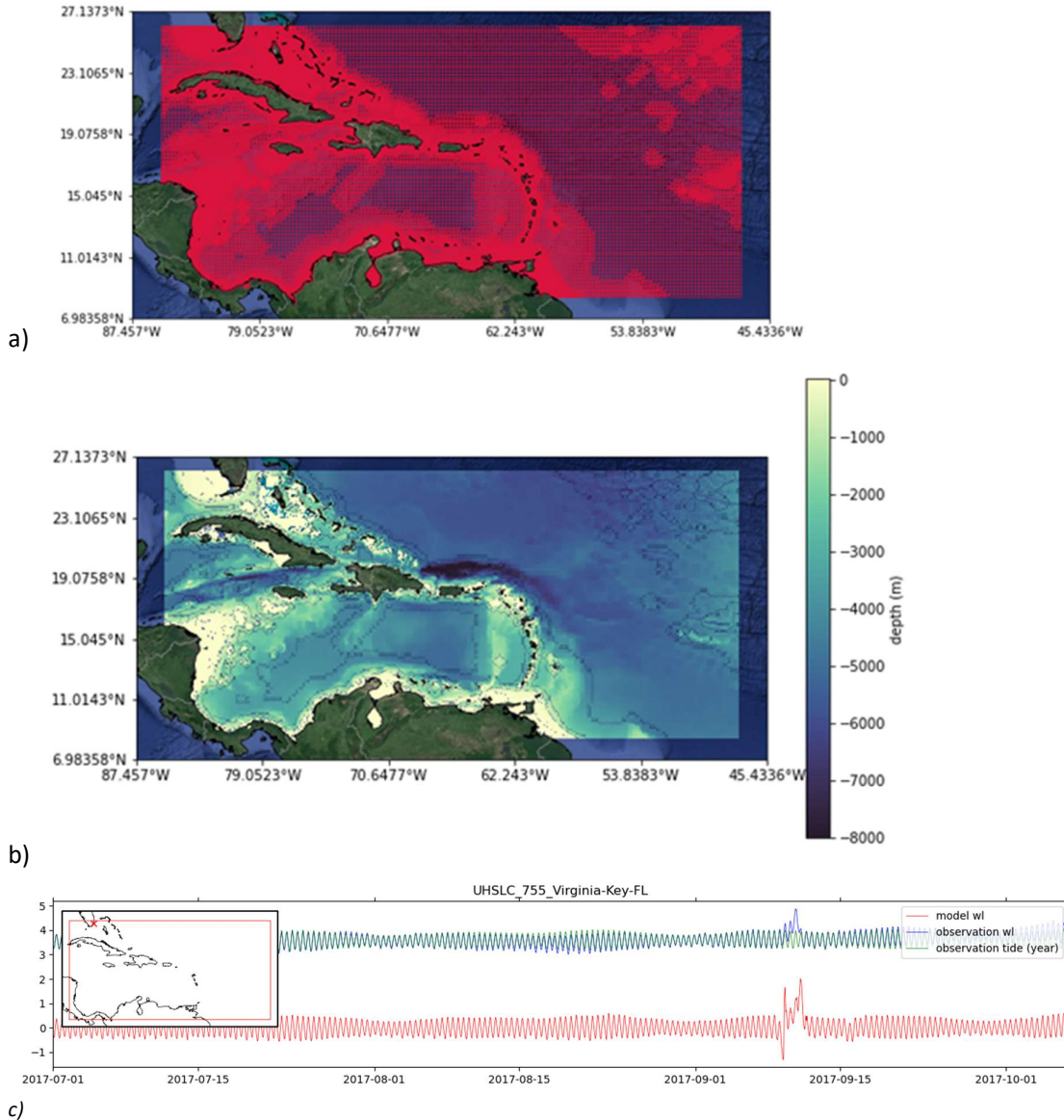


Figure 3.4. Model grid (a) and bathymetry (b) of the hydrodynamic model. Comparison of the observed and modelled water levels (c) at Virginia Key, Florida. The offset is due to a different vertical datum.

HYDROLOGICAL MODEL – WFLOW_SBM

The wflow-sbm hydrological model developed at Deltares was schematized for St. Martin, Martinique and the Dominican Republic (Imhoff et al., 2020; Eilander et al., 2022a). wflow_sbm is a distributed hydrological model developed to maximize the use of high-resolution spatial data from Earth observations. An advantage of the model concept is its flexibility in spatial resolution and its

performance without calibration. Models can be set up (automated) for river basins around the globe using open data at various spatial resolutions, using the Wflow plugin of the HydroMT python package developed by Deltares (Eilander et al., 2022a). The model parameters are estimated from point-scale pedotransfer functions (Imhoff et al., 2020) that relate the model's parameter values to physical system characteristics such as soil type, soil conductivity, etc. The advantage of these pedo-transfer functions is that models can be parameterized based on global datasets and no local calibration is needed. This is especially advantageous in data sparse regions such as the Caribbean Islands where in-situ observations required for calibration are very limitedly available.

For this study the models were set-up at different grid resolutions for the different islands. For the Dominican Republic and Martinique, the models were set up at a regular grid resolution of ~1km that allows for detailed streamflow simulations. Due to the smaller size, for Saint Martin a resolution of ~100m was used. The DEM that was used for the models comes from the MERIT-Hydro dataset (Yamazaki et al. 2019). For the models a threshold of 4 km² (1km² for St Martin) of upstream area was set for rivers to be drawn. The river width was set to a minimum of 30 meters and the depth was estimated with a power law distribution, with a minimum of 1 meter.

The HCLIM dataset was only available for cyclone seasons (June-October). Therefore, the initial state of the wflow-sbm models were created by running the wflow models from June 2007 to June 2017 with meteorologic data from CHIRPS (for the precipitation) and ERA5 (for the potential evapotranspiration).

From the wflow_sbm simulations we use the simulated discharges at the intersection points of the rivers with the SFINCS model grid and the effective precipitation. The effective precipitation is the remaining part of the total precipitation after evapotranspiration, vegetation interception and infiltration have been subtracted in the water-balance component of the hydrological model. This is the water that will runoff and can potentially cause flooding.



Figure 3.5: wflow_sbm modelling domains for the St. Martin. The green shaded areas indicate the entire modelling domain, blue lines are modelled rivers and the lightblue areas indicate lakes. The wflow_sbm domains for the other islands are made in a similar way.

FLOOD MODEL – SFINCS

SFINCS (Super-Fast Inundation of Coasts) is a reduced-complexity model capable of simulating compound flooding with a high computational efficiency balanced with an adequate accuracy. In SFINCS a set of momentum and continuity equations are solved with a first order explicit scheme based on Bates et al. (2010). For more information see Leijnse et al (2020). Here, SFINCS models were

set-up for the 3 case studies, using the SFINCS plugin of the HydroMT python package developed by Deltares (Eilander et al., 2022c).

For each case study a computational grid was defined in the local UTM coordinates and a spatial resolution of 30 m; except for the Dominican Republic for which a 90m resolution was chosen due to the large extent of the domain. Using FABDEM and the latest GEBCO bathymetry (GEBCO-Compilation-Group, 2021), a continuous elevation grid was created for each case study using bilinear resampling. Additionally, a roughness grid was created by using the Copernicus Global Land Service v2 2015 epoch dataset (Buchhorn et al., 2020) and a Manning roughness mapping table. The MERIT-Hydro hydrography dataset (Yamazaki et al. 2019) was used to delineate the rivers' location and ensure good connection with the Wflow-SBM model. The river bathymetry was estimated based on a 1-in-2 year discharge and river width dataset (Lin et al., 2020), using a gradually varying flow algorithm (Neal et al., 2021). To focus on the coastal zone, the active modelling domain of SFINCS was defined using a maximum elevation of 100 m and 30 m for Martinique and St. Martin respectively, while for the Dominican Republic coastal (sub)basins within the area of interest where used to ensure that the modelling domain of SFINCS will not be unnecessarily too large.

For each scenario (evaluation, PGW and PGW+SLR) the boundary conditions created by the GTSM and WFlow models were used to force SFINCS. Since GTSM does not account for waves, here we applied a commonly used assumption for the wave setup, of 20% of the offshore significant wave height H_s (Vousdoukas et al., 2018), which was taken from the closest ERA5 grid points. More specifically, the water level time-series of GTSM ($+ 0.2 \times H_s$) at the closest output locations of each case-study were used to force the SFINCS boundaries, defined at a depth of 5 m, with a weighted average between the 2 closest GTSM points. To ensure that the vertical datums of the water levels, topography and bathymetry are coherent, the global mean dynamic topography map from Andersen et al. (2009) was used. Discharges as calculated in the WFlow model were forced at locations where rivers were flowing in the SFINCS modelling domain. The gridded effective precipitation as calculated in the Wflow model was used to force the SFINCS model with direct rainfall-on-grid over its entire domain. The modelling domains and forcing conditions for each of the 3 case studies are given in Figures 3.6-3.8.

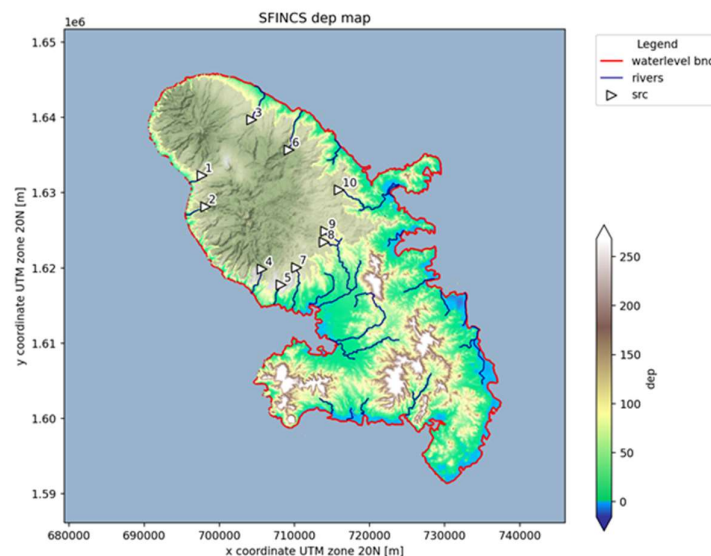


Figure 3.6: Elevation (dep) map for Martinique (in meters). A cut-off elevation of 100 m is used above which the topography is colored grey. The red dots around the island indicate the location of SFINCS coastal boundaries, where the GTSM water levels are forced. The triangles indicated the location where rivers are flowing in the domain (and where the discharges from WFlow are forced), while the blue lines indicate the location of rivers in the domain.

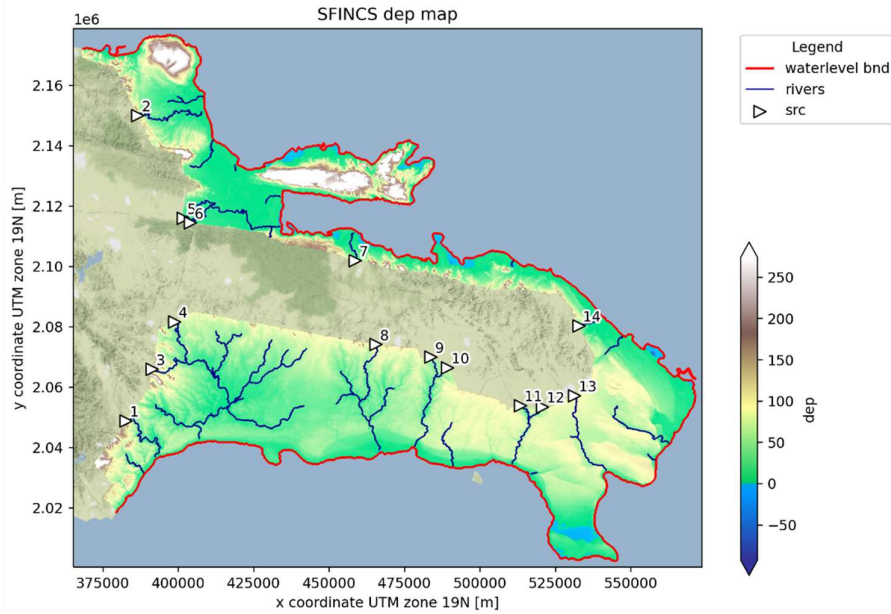


Figure 3.7: Elevation (dep) map for Dominican Republic (in meters). The red dots around the island indicate the location of SFINCS coastal boundaries, where the GTSM water levels are forced. The triangles indicated the location where rivers are flowing in the domain (and where the discharges from WFlow are forced), while the blue lines indicate the location of rivers in the domain.

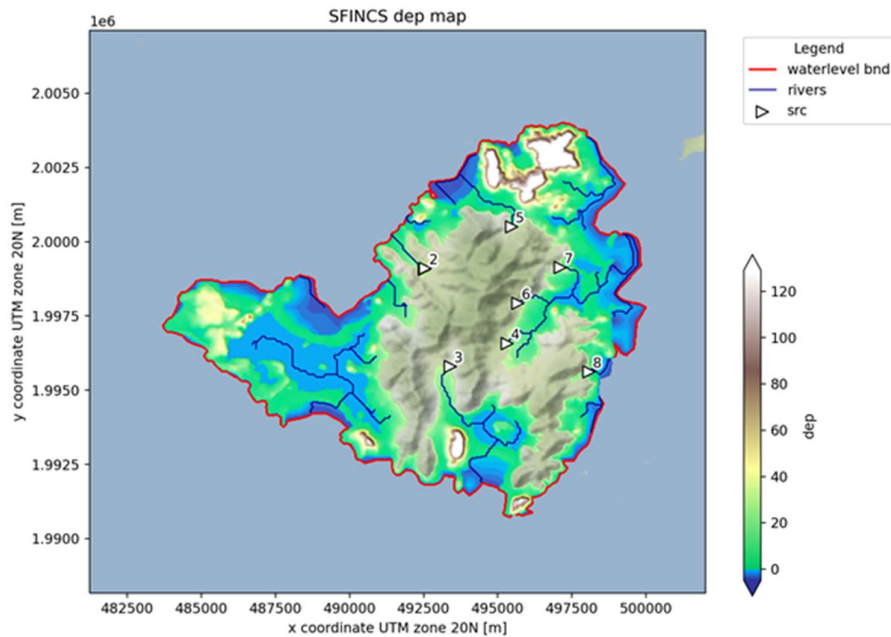


Figure 3.8: Elevation (dep) map for St. Martin (in meters). The red dots around the island indicate the location of SFINCS coastal boundaries, where the GTSM water levels are forced. The triangles indicated the location where rivers are flowing in the domain (and where the discharges from WFlow are forced), while the blue lines indicate the location of rivers in the domain.

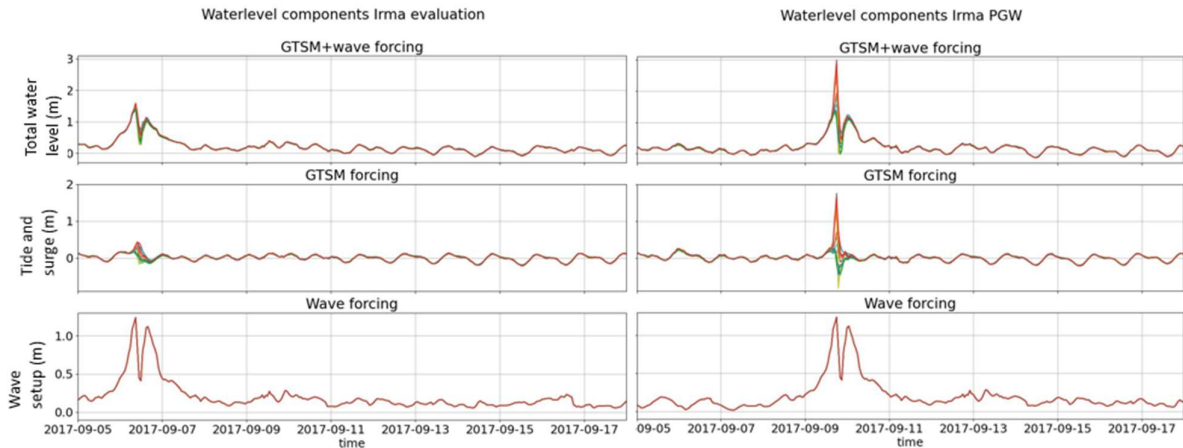


Figure 3.9: The water level forcing for cyclone Irma decomposed into the different components. The upper graph is the total water level, which is the sum of the tide and surge simulated with GTSM and the wave setup calculated from the ERA5 wave data. The lower two graphs are the GTSM forcing (surge and tide) and wave forcing (wave setup), respectively. In the PGW run the wave forcing is shifted in time so the historic peak aligns with the peak in the future PGW HCLIM data.

IMPACT MODEL - FIAT

The Flood Impact Assessment Tool (FIAT) is a flexible open-source toolset developed by Deltares for building and running flood impact models that are based on the unit-loss method (Slager et al. 2016). The tool estimates economic damages, linking flood hazard to exposure data by means of vulnerability information (see fig. 3.10). Here, FIAT models were set-up for the 3 case studies, using the FIAT plugin of the HydroMT python package developed by Deltares (Eilander and Boisgontier, 2022).

The vulnerability curves for residential homes to flooding were derived from a global database including depth-damage factor functions and maximum residential damage estimate per building, both at country level (Huizinga et al., 2017). The depth-damage factor function used was based on a weighted averaged between curves as reported in Huizinga et al. (2017), for different types of assets (residential, industrial, commercial, etc.). Using the building footprint and population data the maximum damage per cell can be calculated based on the population count per cell. Then the expected damage maps are estimates by using the flood depth maps, the damage functions and the maximum damages. It should be noted that the flood depth maps (maximum water depth during the event) as produced from SFINCS are first masked using a water occurrence map (Pekel et al., 2016) to ensure that areas with permanent water are not considered in the damage calculations. Additionally, locations where the maximum flood depth was smaller than 0.1 m, were excluded from the impact calculations. The number of people that are affected by different water depths is calculated as well, using different water depth thresholds. We use the ranges of 0.1 m – 0.25 m, 0.25 m – 0.75 m, 0.75 m – 1.5 m, and > 1.5 m water depths, as proxies to describe people that are affected by minor, intense, major and severe flooding respectively.

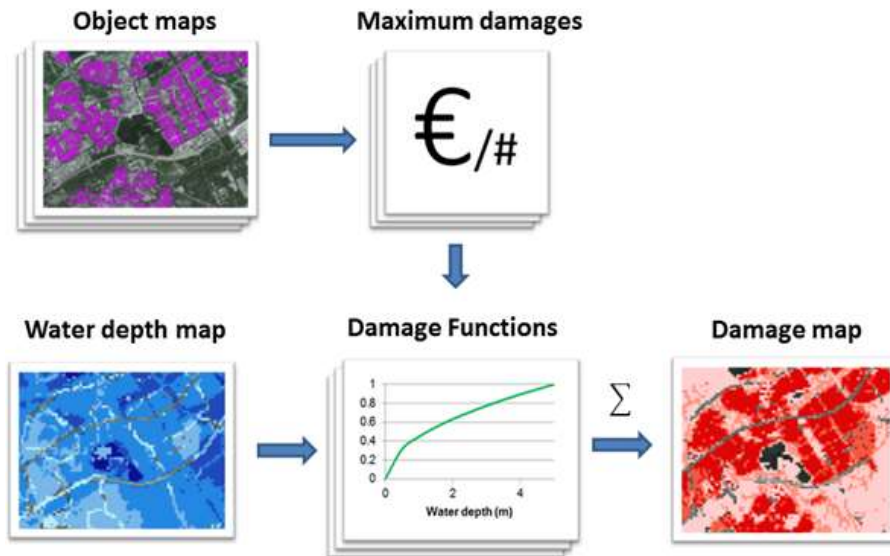


Figure 3.10: Overview of damage calculations in FIAT. Exposure information (“object maps”) are combined with hazard maps (“water depth maps”) via vulnerability functions (“damage function” and “maximum damages”), resulting in “damage maps”.

3.1.4 Data – input and static data used in the modelling chain

HCLIM

To simulate the storm surges, we force the GTSM model with wind speed and atmospheric pressure (u_{10} , v_{10} and psl) from simulations from the HCLIM climate model (Belušić et al., 2020). For the simulation of discharges and effective precipitation with the hydrological model we use temperature, precipitation and radiation (tas , pr and $rsds$) from HCLIM. The model has a spatial resolution of 0.0275° (~ 3 km) and a time resolution of 1 hour. The evaluation run represents the historical period (1979 to now), while the PGW run represents the far future (2090-2099). The simulations are carried out per cyclone season that spans from 1 June to 31 October. The simulations cover the 11 most active cyclone season for both the evaluation and PGW experiments, namely 1980, 1988, 1995, 1996, 1998, 2004, 2005, 2007, 200, 2017 and 2020. Only the boundary conditions and initial states for the CP-RCM are prescribed. Thus, unlike in re-analysis simulations with Numerical Weather Prediction models where data assimilation is applied to ensure that historical simulations resembles the historic observed weather as much as possible, the simulated atmospheric conditions tend to deviate from the observations. As a consequence, the cyclone tracks in the CP-RCM evaluation run will differ from observations as well. In response to the PGW perturbations various factors can change, including the cyclone intensity and track position (warmer seas can sustain intensification with higher wind speeds and lower atmospheric pressure) and associated rainfall (warmer air can hold more moisture). For more details about the climate modelling, we refer the reader to Belušić et al (2020) and EUCP deliverable D3.5.

Digital Elevation Model – FABDEM

Since high-resolution local digital elevation models (DEMs) are not available for the case studies, global products had to be used. There are several global DEMs available measured from space missions. These DEMs can have spatial resolution ranging from approximately 90 m to 30 m at the equator. Unfortunately, these products are mostly surface models which measure the top of buildings or trees. This is problematic for the accuracy of flood simulations derived with these DEMs. To correct these artefacts and produce a global terrain model which better captures the ground elevation, the FABDEM (Forest And Buildings removed Copernicus DEM) was created by the University of Bristol (Hawker et al. 2022). This is a global elevation map that removes building and tree height biases from the Copernicus GLO 30 Digital Elevation Model (COPDEM30) and is available at 1 arc second grid spacing (approximately 30m at the equator). FABDEM reduces mean absolute vertical error in built-up areas from 1.61 to 1.12 m, and in forests from 5.15 to 2.88 m relative to COPDEM30. This DEM was used for the compound flood modelling described in section 3.1.3.

Population data

In order to translate the flood maps that are produced in the present study to actual impacts, exposure maps are needed. To this end, the WorldPop data (<https://www.worldpop.org/geodata/listing?id=79>) were used to describe the distribution of the population in the case study areas. More specifically, the constrained gridded population count datasets (~ 100 m resolution) of 2020 were used, with country totals adjusted to match the corresponding official United Nations population estimates (2019 Revision of World Population Prospects) (Bondarenko et al. 2020). To account for the local spatial distribution of the population, the World Settlement Footprint (WSF-2015) (Palacios-Lopez et al., 2019) dataset was used, which has a ~ 10 m resolution, to identify the build-up footprint. This resulted

in a more accurate spatial allocation of the population from the WoldPop dataset. More information is provided in the section on impact modelling (3.1.3.4).

ERAS

For the hydrological modelling the historical temperature and potential evaporation data were calculated from the global gridded re-analysis dataset ERA5² (Hersbach et al., 2020) that is produced by the European Centre of Medium-Range Weather Forecasting (ECMWF). ERA5 temperature data was further downscaled from the original 0.25° grid to the 1x1 km grid of the wflow model using the MERIT hydro high-resolution digital elevation model (Yamazaki et al., 2019) and a lapse rate of -0.0065°C/m. Potential evaporation was estimated using ERA5 radiation and the downscaled temperature data in the formula of de Bruin (de Bruin et al., 2016). Also estimates of waves component of extreme sea level were obtained from ERA5. The wave setup at the coast was estimated to be 20% of the significant height of combined wind waves and swell (Vousdoukas et al., 2018). Since producing wave simulations for the PGW scenario was out of the scope of this study, it was decided to use the historic wave data from the ERA5 reanalysis in the PGW runs, assuming the same wave forcing in the future for the individual cyclones. This assumption is further discussed in Section 3.1.5.

CHIRPS

The precipitation input of the hydrological model was taken from the CHIRPS dataset. The CHIRPS dataset is a 35+ year quasi-global rainfall data set (Funk et al., 2015). It spans 50°S-50°N (and all longitudes) and ranges from 1981 to near-present, CHIRPS incorporates a rainfall climatology, 0.05° resolution satellite imagery, and in-situ station data to create gridded rainfall time series that are available in near-real time. The data for the period June 2007 to June 2017 were used.

SEA LEVEL RISE SCENARIOS

The pseudo-global warming (PGW) simulations provided by EUCP partner KNMI assume an increase of temperature of 2 degrees Celsius. This roughly corresponds with a relatively optimistic climate scenario SSP1-2.6 scenario in 2100 (IPCC, 2021). For this emission scenario, the IPCC projects a global mean sea level rise (SLR) of approximately 0.6 meter with the respect to 1900. The SLR was added to the coastal boundary conditions for the PGW+SLR runs. SLR may vary regionally, and it is projected that the Caribbean may experience higher SLR than the global mean, but here it was assumed that the global mean SLR is representative for regional changes in the Caribbean.

3.1.3 Results

3.1.3.1 METEO

The HCLIM meteo variables of main relevance for tropical cyclones are wind speeds, air pressure and precipitation. The (difference between the) evaluation and PGW runs are depicted in Fig. 3.11 to 3.14 for each of the tropical cyclones. These spatial plots clearly show the shifts in tropical cyclone path between the evaluation and PGW datasets and their deviation from the IBTrAC measured cyclone

² cds.climate.copernicus.eu/cdsapp#!/dataset/reanalysis-era5-pressure-levels?tab=overview

track (see also section 3.1.4 HCLIM). In order to still be able to compare the evaluation and PGW datasets, the data is aggregated over the whole domain and in the period of the cyclone in Fig. 3.15. These aggregated values mostly show more extreme values for the PGW dataset compared to the evaluation, namely higher maximum wind speeds, lower pressures and higher precipitation intensities and depths.

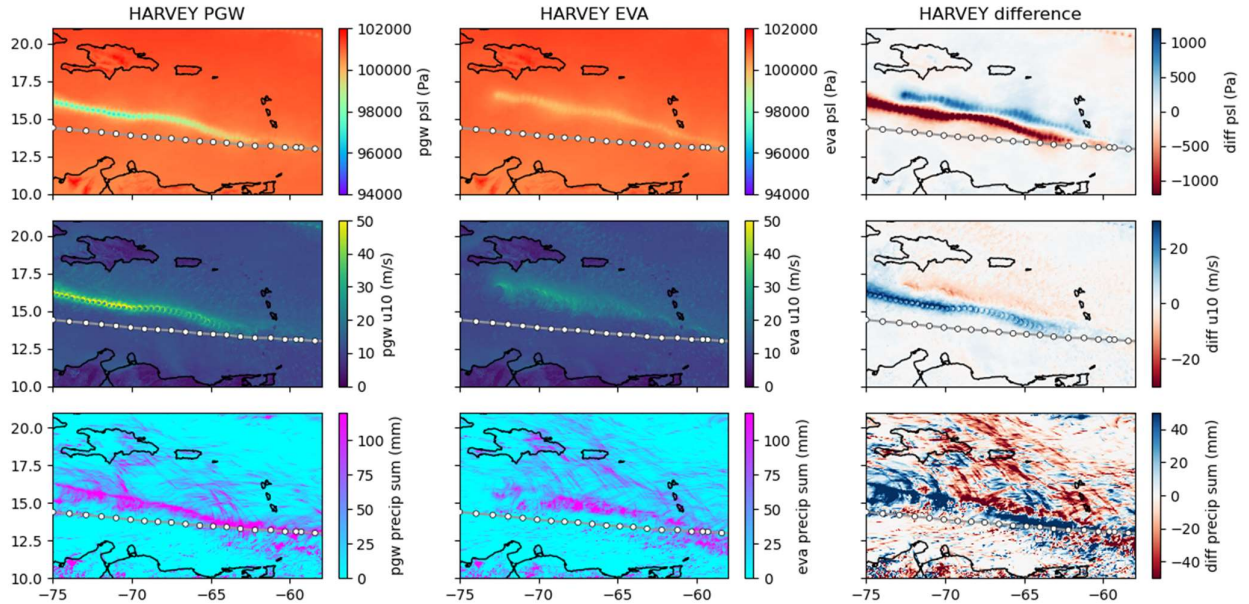


Figure 3.11: Minimal air pressure (top row), maximum wind speed (middle row) and total precipitation (bottom row) during tropical cyclone Harvey. Dotted line presents the IBTrAC measured cyclone track. Difference in the right subplot represents PGW minus EVA values from the left and middle subplots.

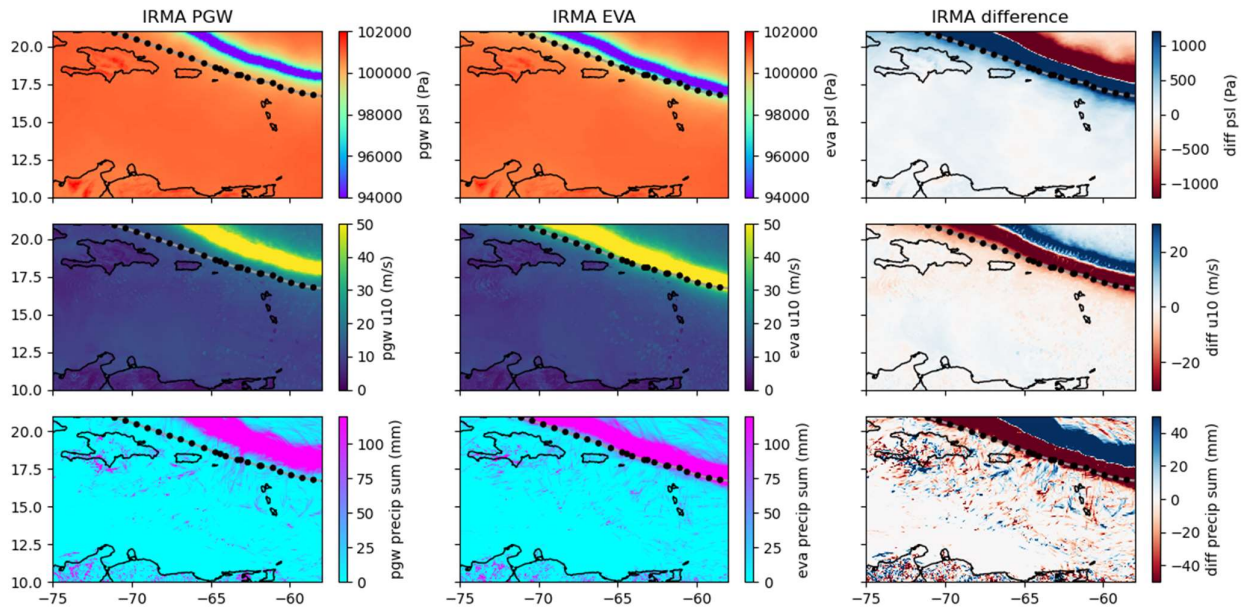


Figure 3.12: Minimal air pressure, maximum wind speed and total precipitation during tropical cyclone Irma. Dotted line presents the IBTrAC measured cyclone track. Difference in the right subplot represents PGW minus EVA values from the left and middle subplots.

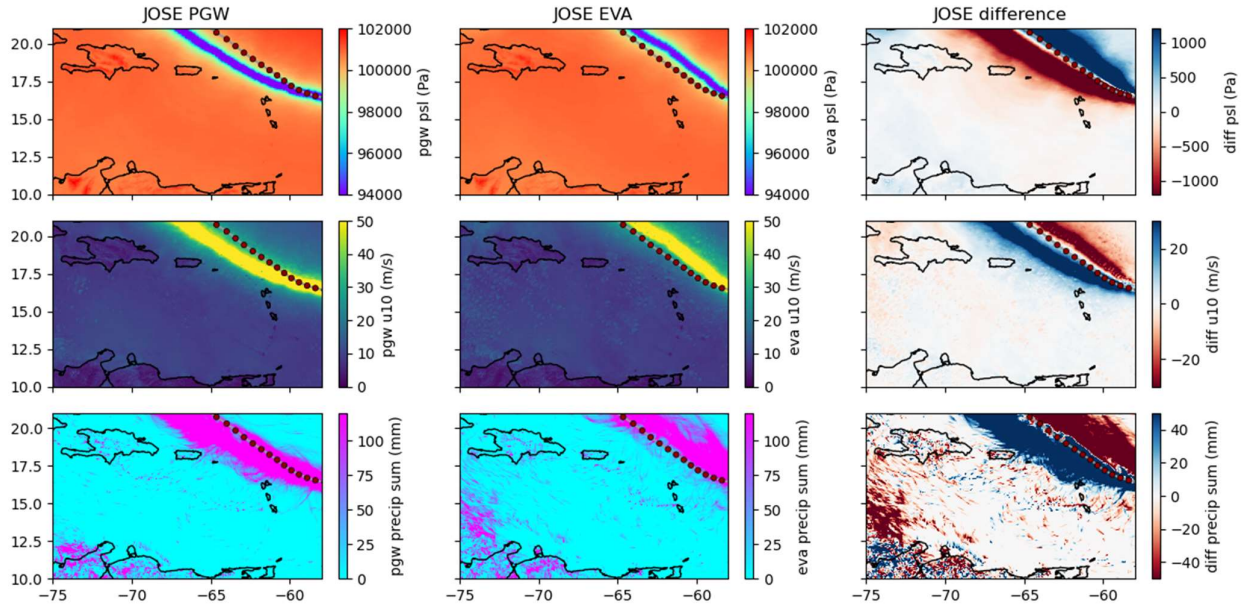


Figure 3.13: Minimal air pressure (top row), maximum wind speed (middle row) and total precipitation (bottom row) during tropical cyclone Jose. Dotted line presents the IBTrAC measured cyclone track. Difference in the right subplot represents PGW minus EVA values from the left and middle subplots.

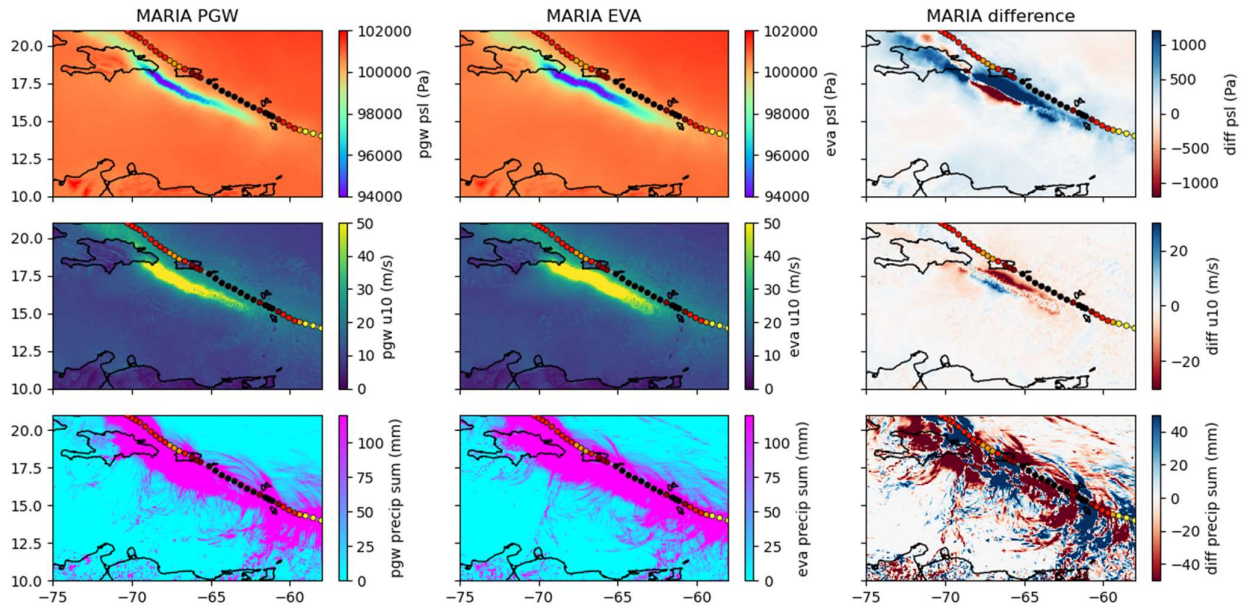


Figure 3.14: Minimal air pressure (top row), maximum wind speed (middle row) and total precipitation (bottom row) during tropical cyclone Harvey. Dotted line presents the IBTrAC measured cyclone track. Difference in the right subplot represents PGW minus EVA values from the left and middle subplots.

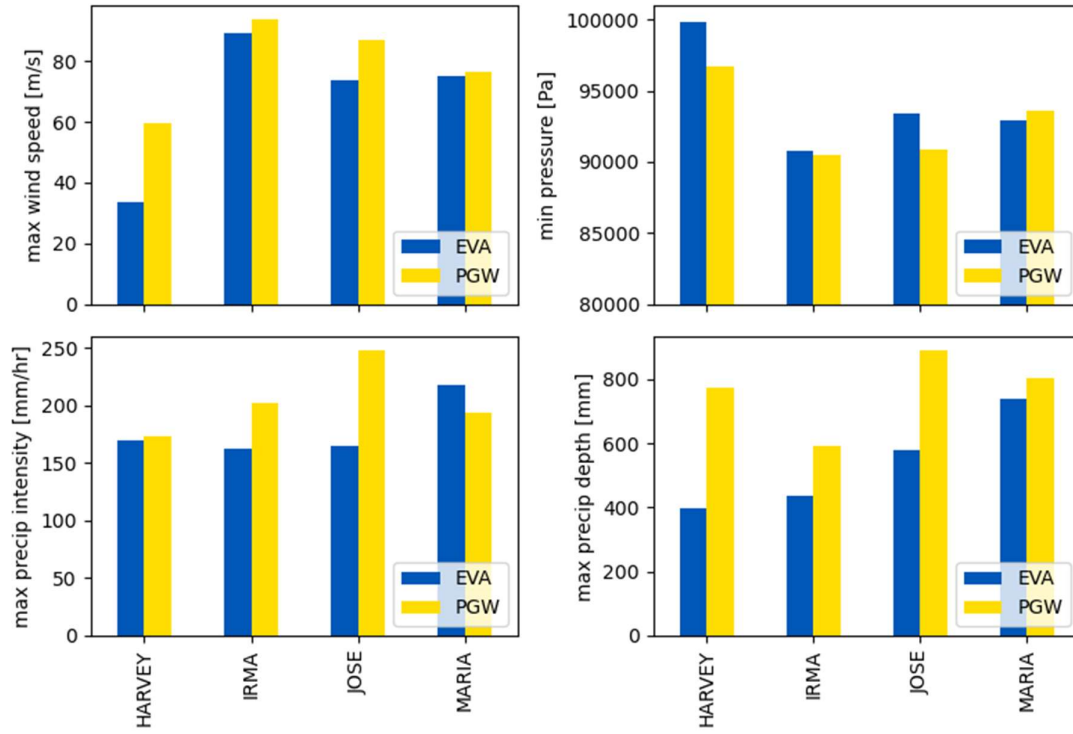


Figure 3.15: Aggregated values for four tropical cyclones in 2017. Maximum wind speed (max over time and of the domain), minimum pressure (min over time and of the domain), maximum precipitation intensity (max over time and of the domain) and maximum precipitation depth (sum over time, max of the domain) per cyclone event.

3.1.3.2 GTSM

For each of the four cyclones we analysed the change in maximum storm tide between the evaluation and PGW run. Figure 3.16 summarizes the results and shows the maximum still water levels (storm surge plus tides) obtained from GTSM and the significant wave height obtained from ERA5, for each of the events. Changes in the cyclone track between the evaluation and PGW run were to be expected due to the warmer seas and atmospheric conditions that cause changes in wind speed and atmospheric pressure. A change in cyclone propagation speed can affect the wind fetch and consequently change in storm surge and wave action. The stalling of a cyclone can be destructive as strong winds last longer, the storm surge and wave action stay high, and rain keeps falling in the same place. Since storm surge height are defined by the bathymetry and coastline geometry (besides wind speed and pressure), even a minor shift in the cyclone track can result in a locally large change in water level.

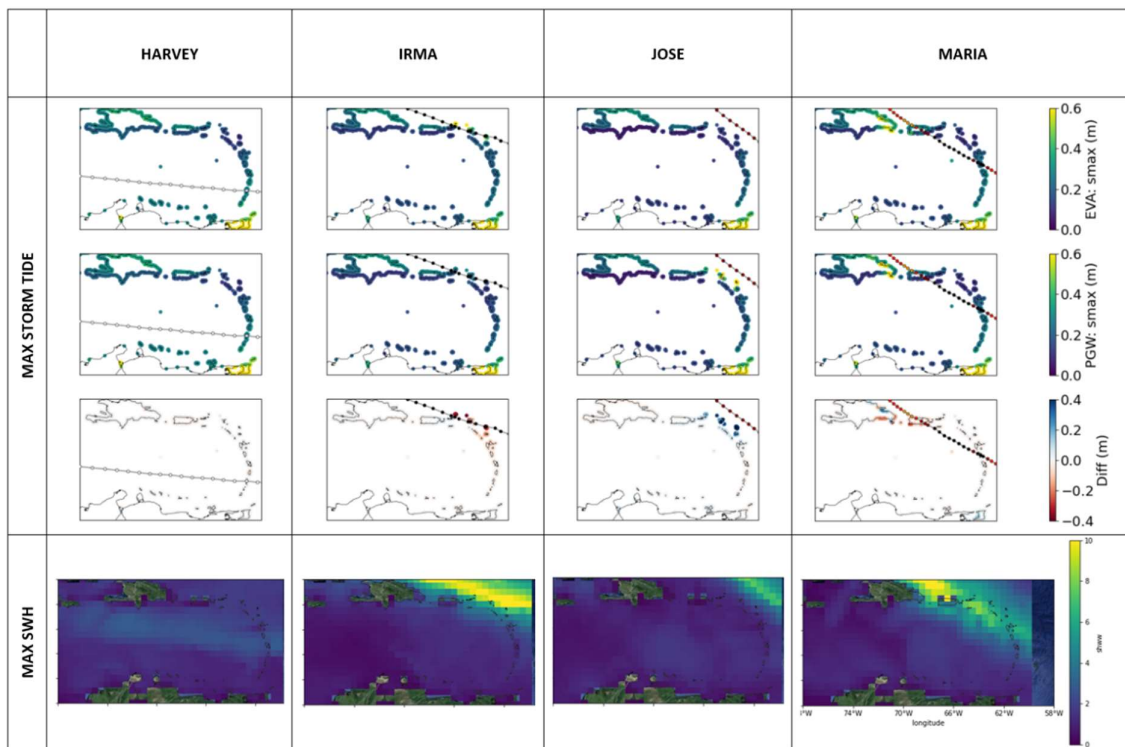


Figure 3.16: Maximum water levels (storm surges and tide) and maximum significant wave heights for four selected cyclones. The line indicates the observed cyclone track obtained from IBTRCS.

Cyclone Harvey only gained cyclone force after crossing the Gulf of Mexico and crossed the Lesser Antilles as a tropical storm. Consequently, wind speeds were relatively low. A storm surge of 0.2 m occurred near Martinique. Also, the ERA5 significant wave heights are relatively small and below 3 m. When comparing the evaluation and PGW run, the cyclone tracks more north and intensifies more rapidly in the PGW run (Fig. 3.16). However, the area near Martinique with the highest storm surges is located close to the boundary, and there the differences between the two runs are minor.

Cyclone Irma crossed just north of Puerto Rico. Significant wave heights exceed 10 metres for a large part of the Lesser Antilles. In the evaluation run, still water levels exceed 0.6 metres north of the observed track (Figure 3.16), while water levels derived from the PGW run are much lower. From Figure 3.16 it can be observed that the track shifted north further away from the Puerto Rico and neighbouring islands, and thereby diminishing the impact of the cyclone in the Caribbean region.

Cyclone José was a Category 4 cyclone (209–251 km/h) when crossing north of the Leeward Islands. In the evaluation run the maximum surge height was below 0.2 m. Offshore significant wave heights go up to 8 m, just north of the Leeward Islands. In the evaluation run the eye was tracking south of the observed track, while in the PGW run it moved north of the observed track. This completely changed the oceanic response, resulting in much higher storm surges (+0.4 m – see Figure 3.17) in Sint Martin and neighbouring islands.

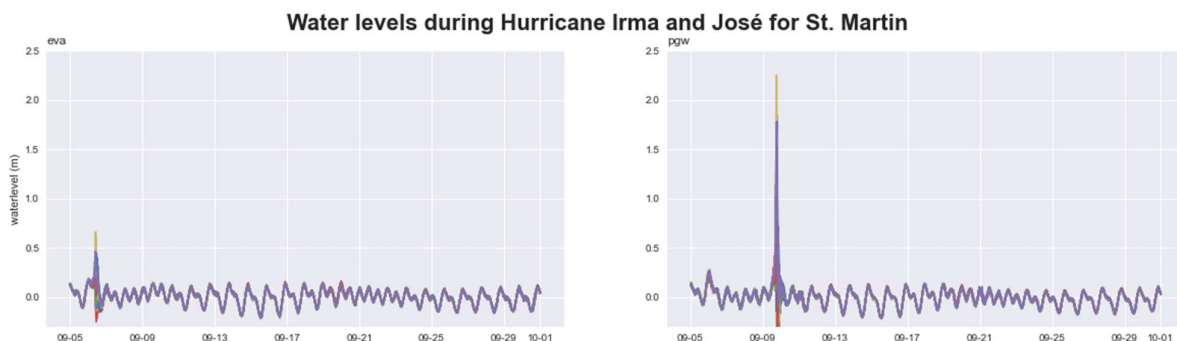


Figure 3.17: Water levels of Cyclone Irma and José for St. Martin at the GTSM output locations (represented by the different colours) along the coast line of St. Martin for the Evaluation scenario (left) and PGW scenario (right).

Cyclone Maria made landfall at Puerto Rico as a Category 5 cyclone (with windspeeds in excess of 252 km/h). In the evaluation run, the maximum still water level is exceeded 1.5 m on the east coast of the Dominican Republic (see Fig. 3.18). This concurred with very high significant wave heights going up to 12-15 m for the region north of Puerto Rico and Dominican Republic. In the PGW run, the track shifted north and increases in size. Maximum water levels increased with 0.4 meters, but other parts of the coastline see a decrease of similar size.

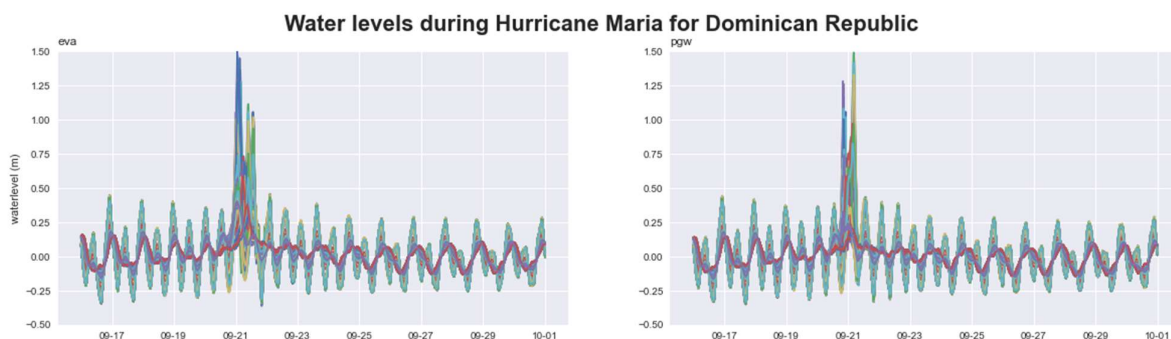


Figure 3.18: Water levels of Cyclone Maria for the Dominican Republic at the GTSM output locations (represented by the different colours) along the coast line of St. Martin for the Evaluation scenario (left) and PGW scenario (right).

3.1.3.3 SFINCS

Martinique – Harvey

Evaluation

Cyclone Harvey hit the island of Martinique on the 19th of August 2017. Figure 3.19 displays the coastal water levels, river discharges and mean precipitation for Martinique.

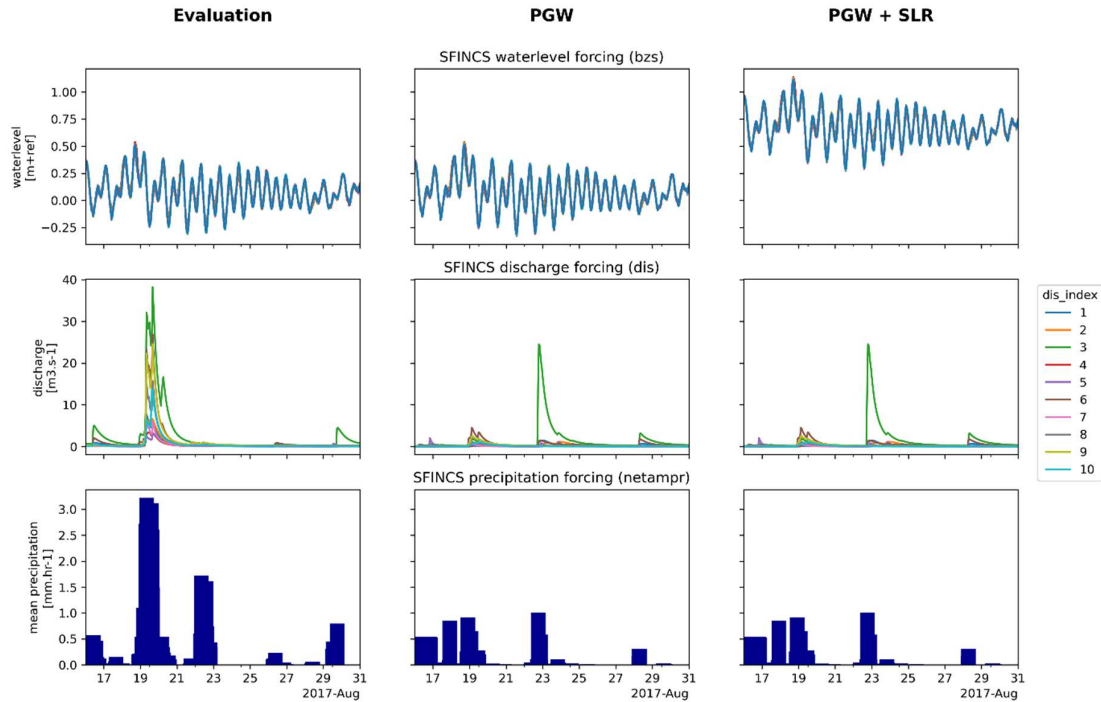


Figure 3.19: Forcing conditions used for the SFINCS model of Martinique for 3 scenarios of cyclone Harvey. The first row shows the water level forcing at island boundaries (different colours represent different GTSM locations, which for the case of Martinique are quite similar since the water levels are dominated by the tides and Harvey was not that strong when it passed from Martinique). The second row presents the discharges at each incoming river location as shown in Figure 3.6. The 3rd row shows the mean effective precipitation across the island. The 3 columns present the 3 different scenarios modelled herein, with the evaluation run, the PGW run and the PGW, including SLR respectively.

In the evaluation run the effective precipitation reached a peak of about 3 mm per hour (Fig. 3.19 - bottom left panel). Also, in the discharges of the rivers that enter the SFINCS domain, a large peak is visible of about 40 m³/s (Fig. 3.19 - middle left). For the sea levels, there is a peak visible as well, which is however only about 0.2 meter higher than the tidal signal (Fig. 3.19 - top left). These forcings result in some small areas being flooded. The flooded areas are mainly located in the southern part of the island. Most of the flooded area is located at higher elevation and is therefore not caused by the water levels on the ocean but mainly by the discharges from the rivers and direct intense precipitation, flooded areas are however small. In the western bay in the middle of the island we do see a larger coastal area that has been flooded, which is probably caused by the combination of large discharges, intense local rainfall and high water levels in the ocean as well.

PGW

For the PGW run (Fig. 3.19 – middle column) shows that the effective precipitation had peaks of about

1 mm/hr, therefore being almost three times as small as in the evaluation run. The total effective precipitation is less intense and more spread over several days. Both the character of the event and its position have changed in the HCLIM PGW simulations. Therefore, the discharges that force the SFINCS model are smaller than in the evaluation run, reaching about 5 m³/s for most rivers, with one exception of 20 m³/s. The water levels do not differ much from the evaluation run, this can be explained by the fact that most of the signal from the GTSM is caused by the tides, which stay the same in the pseudo global warming scenario. The peak that we see in the forcing signal is mostly caused by an increase in the wave setup, from which we do not have data for the future scenario and we therefore use the historical ERA5 data.

Due to the less intense rainfall and lower discharges, there is less flooding in the PGW run than in the evaluation run, both in the higher elevated areas as in the western bay, that is flooded in the evaluation run. Adding the sea level rise to the PGW run slightly increases the coastal flooding in the western bay of the island, flood extents are still smaller than in the evaluation run though.

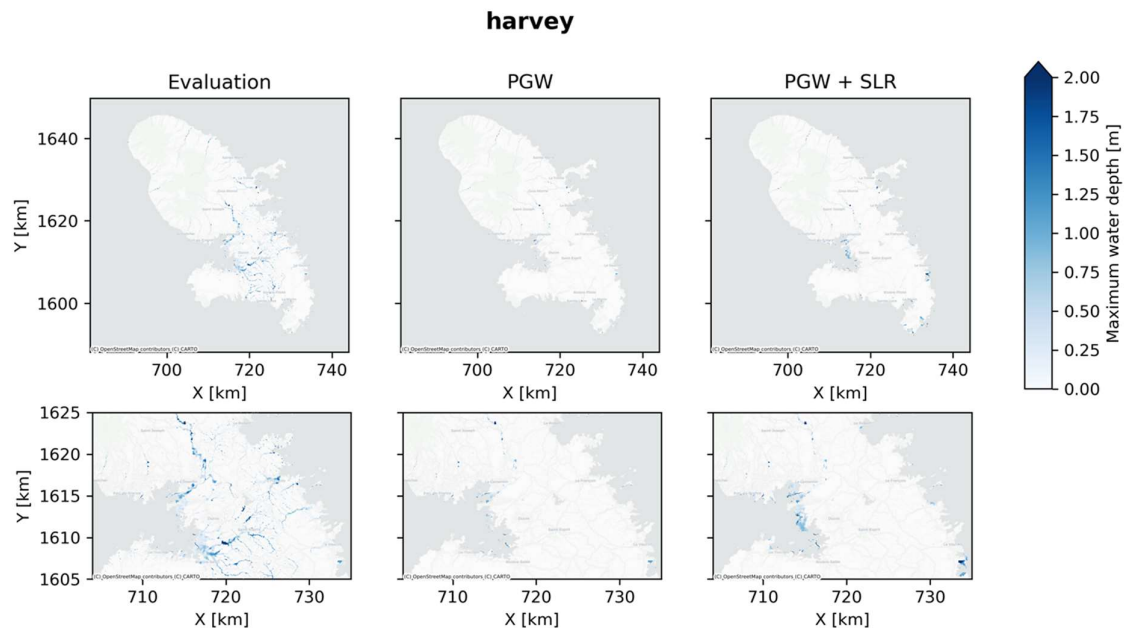


Figure 3.20: Maximum flood depth maps produced with SFINCS for Martinique for 3 scenarios of cyclone Harvey. The 3 columns present the 3 different scenarios modelled herein, with the evaluation run, the PGW run and the PGW, including SLR respectively. The top row maps include the whole of Martinique, while the bottom row maps present a zoom in area that includes Fort-de-France. Flood depths < 0.1 m have been masked for visualization purposes.

harvey

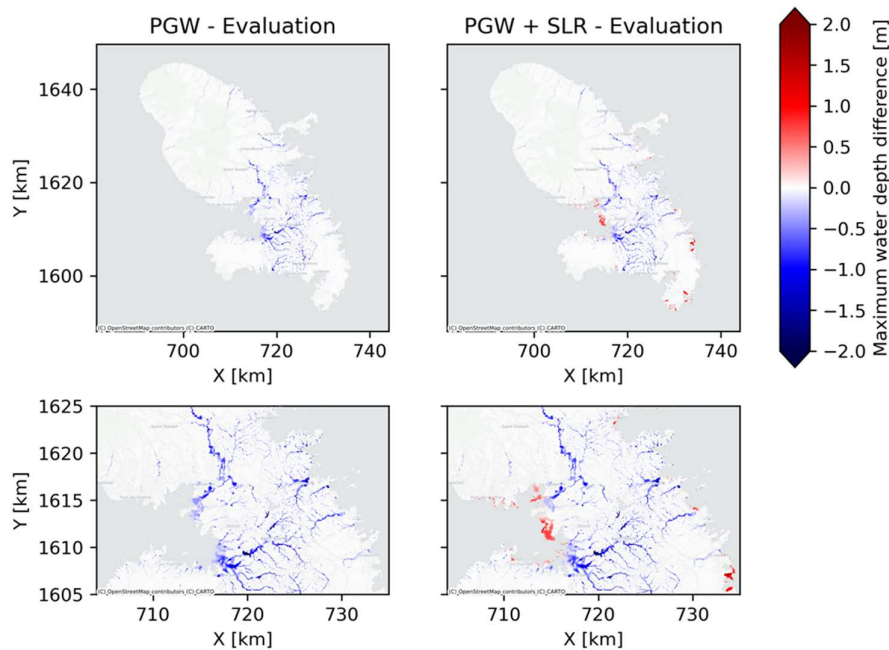


Figure 3.21: Maximum flood depth difference maps for Martinique between the PGW (+SLR) runs and the evaluation run of cyclone Harvey. The top row maps include the whole of Martinique, while the bottom row maps present a zoom in area that includes Fort-de-France.

Dominican Republic – Maria

Evaluation

Cyclone Maria affected the Dominican Republic as it tracked northeast of the country on the 21st of September 2017. In the evaluation run the peak of the mean effective precipitation in the SFINCS modelling domain reached values of more than 10 mm per hour (Fig. 3.22). Additionally, since there are large rivers entering the SFINCS modelling domain, discharges peaks reached values of about 7,000 m³/s in the northern part of the domain. The water level time-series differed along the coastline, with high contributions from the wave-setup and total water levels reaching values of around 2.3 m at some locations.

The combined effect of the previously described processes resulted in SFINCS predicting quite some areas to be flooded (Fig. 3.23). These included high water depths in the northern parts of the domain, where the Yuna river reaches the coast; and in the southern part where Santo Domingo is located, and where different rivers meet. In the eastern part of the domain flooding is mainly caused by increased precipitation.

PGW

In the PGW run, the cyclone track shifted North (Fig. 3.14). This resulted in an increase of the storm surge height by even 0.4 m at some locations, but since the main contribution of the water levels comes from the wave setup (which stays the same between the evaluation and PGW runs, since we assume the same wave forcing from ERA5), the general changes from coastal flooding were not high. However, the shift led to increased precipitation in the northern part of the domain and slightly higher

water depths on average (Fig. 3.23 and 3.24). On the other hand, the rest of the domain had on average smaller water depths due to less intense rainfall and incoming river discharges.

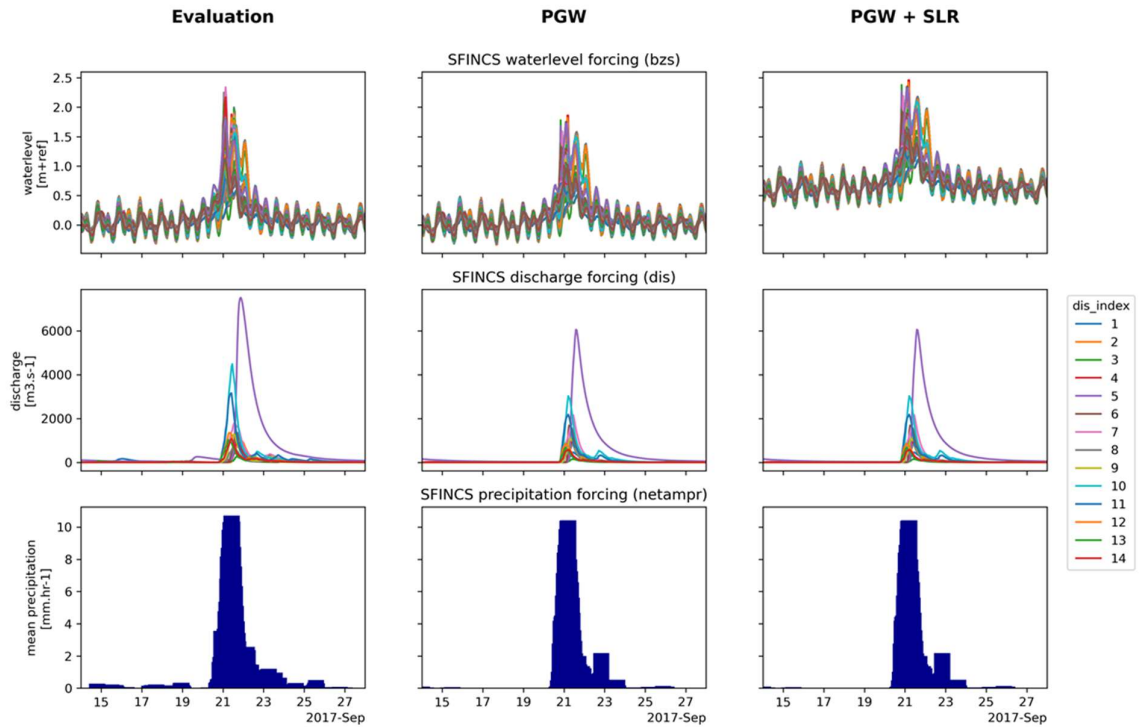


Figure 3.22: Forcing conditions used for the SFINCS model of Dominican Republic for 3 scenarios of cyclone Maria. The first row shows the water level forcing at island boundaries (different colours represent different GTSM locations, which for the case of Martinique are quite similar). The second row presents the discharges at each incoming river location as shown in Figure 3.6. The 3rd row shows the mean effective precipitation across the island. The 3 columns present the 3 different scenarios modelled herein, with the evaluation run, the PGW run and the PGW, including SLR respectively.

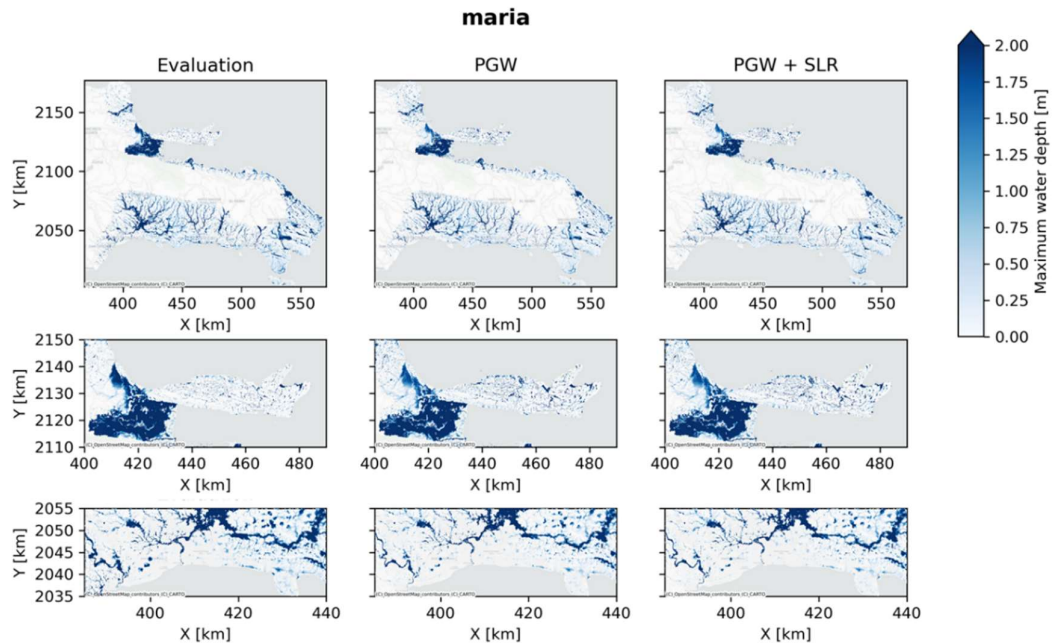


Figure 3.23: Maximum flood depth maps produced with SFINCS for Dominican Republic for 3 scenarios of cyclone Maria. The 3 columns present the 3 different scenarios modelled herein, with the evaluation run, the PGW run and the PGW, including SLR respectively. The top row maps include the whole of Dominican Republic, while the middle and bottom row maps present two zoom-in areas in the northern and southern parts. Flood depths < 0.1 m have been masked for visualization purposes.

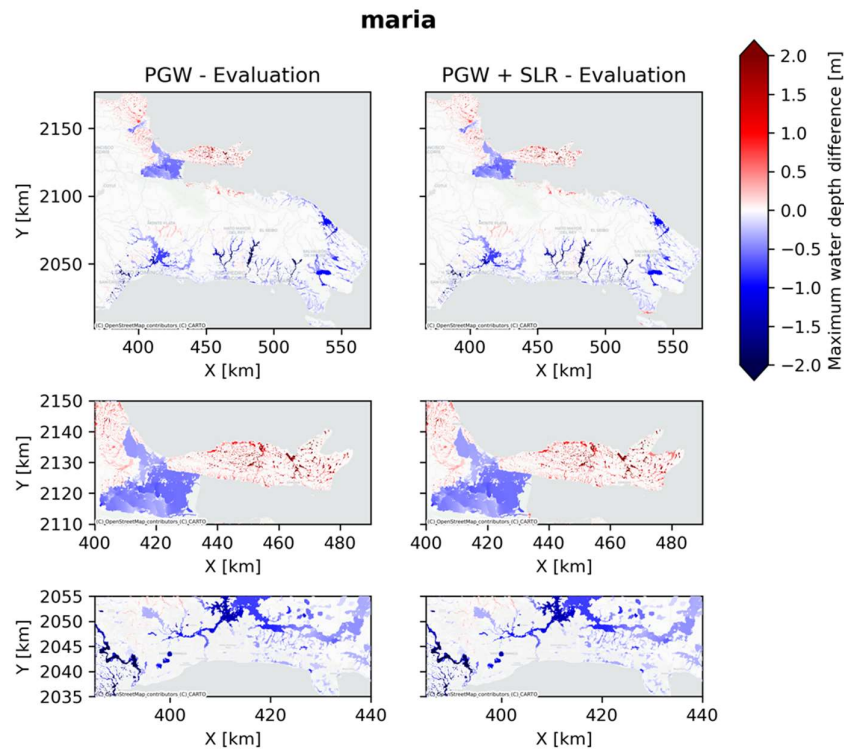


Figure 3.24: Maximum flood depth difference maps for Dominican Republic between the PGW (+SLR) runs and the evaluation run of cyclone Maria. The top row maps include the whole of Dominican Republic, while the middle and bottom row maps present two zoom-in areas in the northern and southern parts.

St. Martin – Irma

Evaluation

Cyclone Irma affected the island of Saint Martin on the 6th of September 2017. The track went almost straight over the island (Fig. 3.15). In figure 3.25 we can see that on the 6th of September the water level in the ocean reached a peak of about 1.5 meter. The discharge reaches levels of approximately 10 m³/s for the largest rivers and the effective precipitation reaches a sharp peak of 10 mm/hr. These forcings resulted in significant flooding, mainly concentrated around the different lakes and some coastal areas in the North and Northwest of the island. Flood depths can be up to 1.5 meters.

PGW

In the PGW experiments the HCLIM model only simulates a small peak in the precipitation on the 6th of September. This is possibly a result of the changed position of the cyclone track that is now further away from the Island. The precipitation peak only reaches about 2-3 mm/hr and is thus almost four times smaller than in the evaluation run. For the water levels and discharges we do not see significant increases on the 6th of September. On the 9th of September, another very large peak is visible with effective precipitation rates of 25 mm/hr, river discharges reaching over 40 m³/hr and a water level that reaches almost 3 meters high in some places. This second peak is the result of cyclone Jose, whereas the first peak on the 6th of September is caused by Irma. The track of Irma moved towards

the north, therefore not hitting the island of St. Martin as directly as in the evaluation run. Jose on the other hand moved more southward, causing the track to be much closer to the island in the PGW run than in the evaluation run.

Since we are using historical (ERA5) wave data to add to the GTSM output, the second peak of Jose was not present in the wave data for the PGW run. To account for this, the highest peak in the wave data was shifted in time so it coincided with the highest peak in the GTSM output. These forcings caused severe flooding in large parts of the coast. The flooding is concentrate around the lakes in the south and west of the island, as well as on the coasts at the northern end of the island. Water depths can exceed 2 meters. In addition, the areas around the largest rivers are flooded as well. For the sea level rise scenario, flood extents are similar to the PGW run, with water depths at the coast being slightly higher.

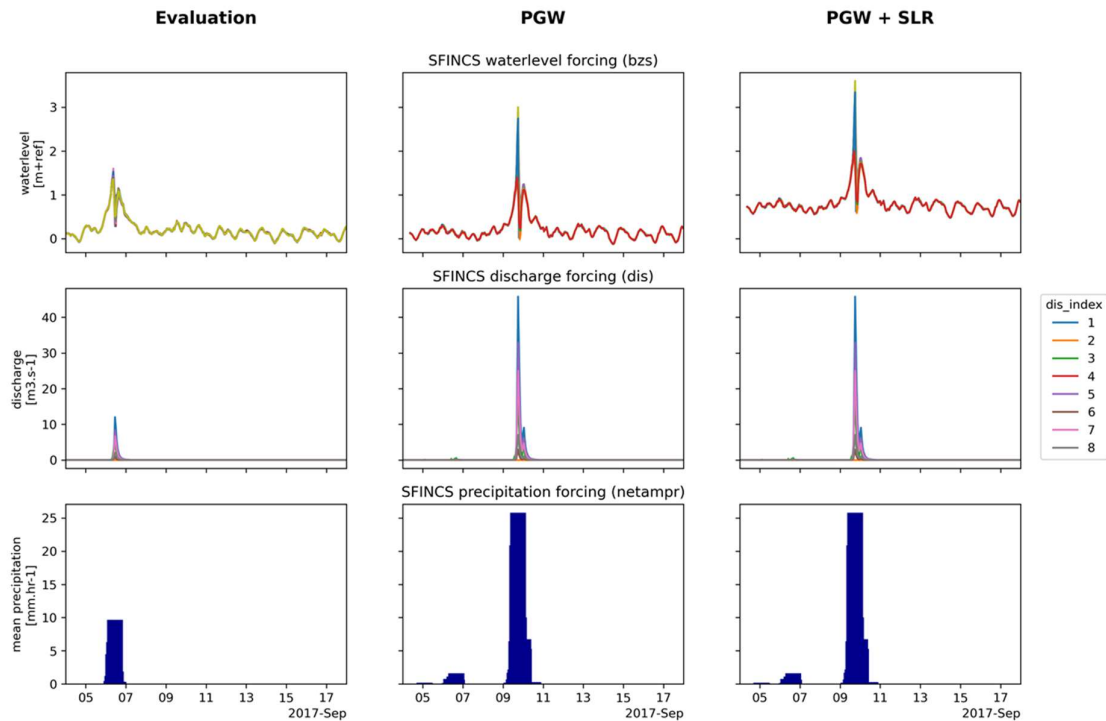


Figure 3.25: Forcing conditions used for the SFINCS model of St. Martin for 3 scenarios of cyclone Irma. The first row shows the water level forcing at island boundaries (different colours represent different GTSM locations, which for the case of Martinique are quite similar). The second row presents the discharges at each incoming SFINCS river location. The 3rd row shows the mean effective precipitation across the island. The 3 columns present the 3 different scenarios modelled herein, with the evaluation run, the PGW run and the PGW, including SLR respectively.

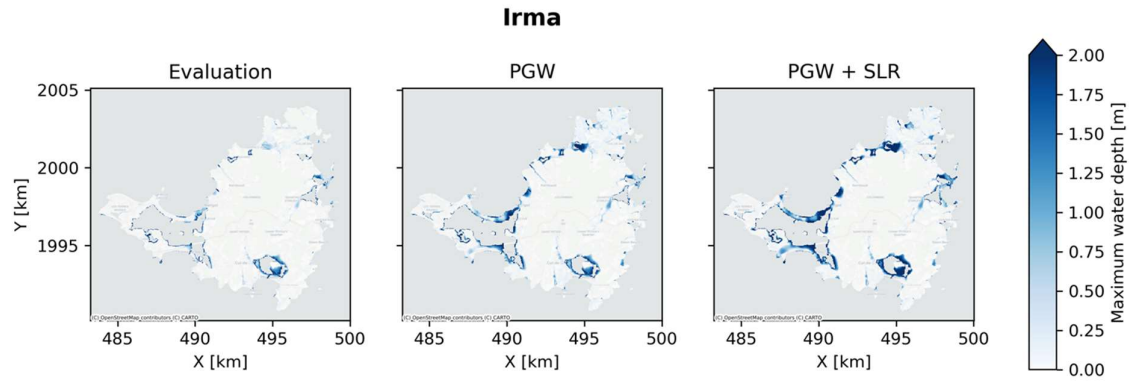


Figure 3.26: Maximum flood depth maps produced with SFINCS for St. Martin for 3 scenarios of cyclone Irma. The 3 columns present the 3 different scenarios modelled herein, with the evaluation run, the PGW run and the PGW, including SLR respectively. Flood depths < 0.1 m have been masked for visualization purposes.

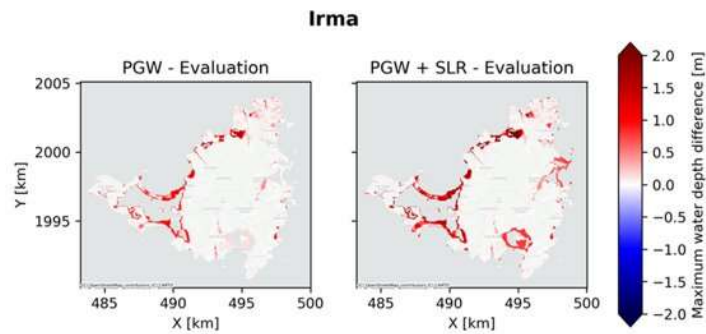


Figure 3.27: Maximum flood depth difference maps for St. Martin between the PGW (+SLR) runs and the evaluation run of cyclone Irma.

3.1.3.4 FIAT

Martinique

For the evaluation run, most damages modelled with FIAT (Figure 3.28) are concentrated in areas around rivers, where high flood depths were calculated (see Figure 3.20). Various areas in Fort-de-France (central west part of the island) and Le François (central east part) show large damages. In the PGW run, these damages drop significantly, with the total damage estimates for the whole island being almost 8 times smaller (Figure 3.29). When SLR is included in the PGW run, the extra flooding in some coastal areas in Fort-de-France results in an increase in damage, which more than doubles the total damages relative to the PGW run without SLR.

As expected from the damage calculation, less people are affected in the PGW runs when compared to the evaluation run (Figure 3.29). For all scenarios, people are mostly affected by water depths smaller than 0.75 m.

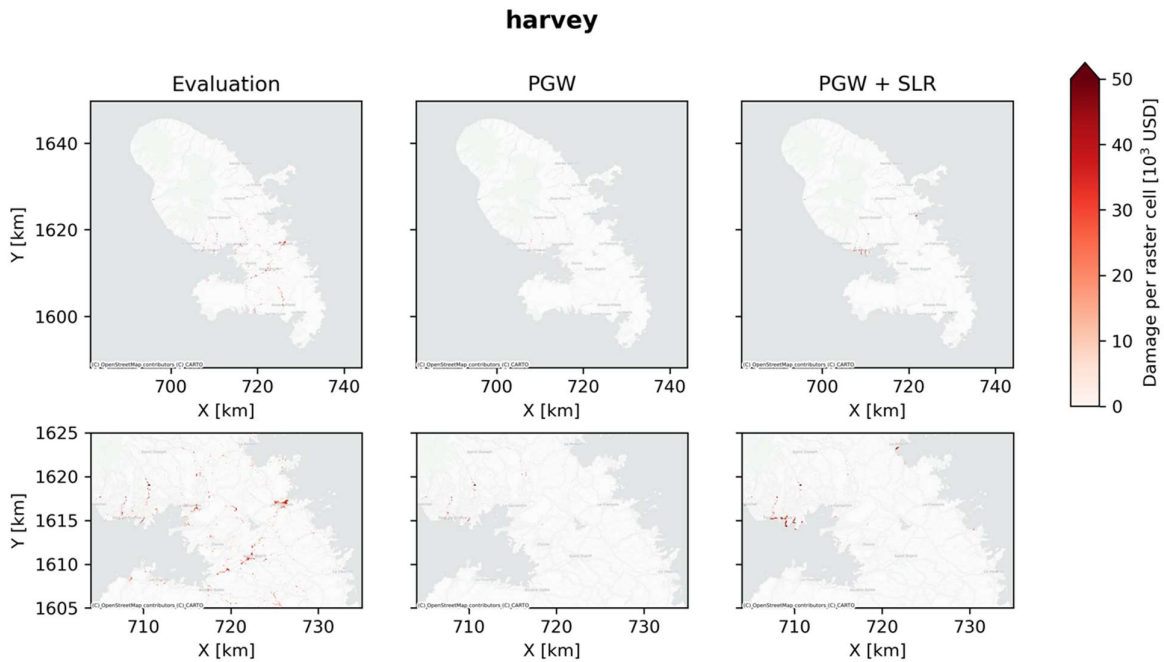


Figure 3.28: Damage maps in USD produced with FIAT for Martinique for 3 scenarios of cyclone Harvey. The 3 columns present the 3 different scenarios modelled herein, with the evaluation run, the PGW run and the PGW including SLR respectively. The top maps include the whole of Martinique, while the bottom maps present a zoom in area.

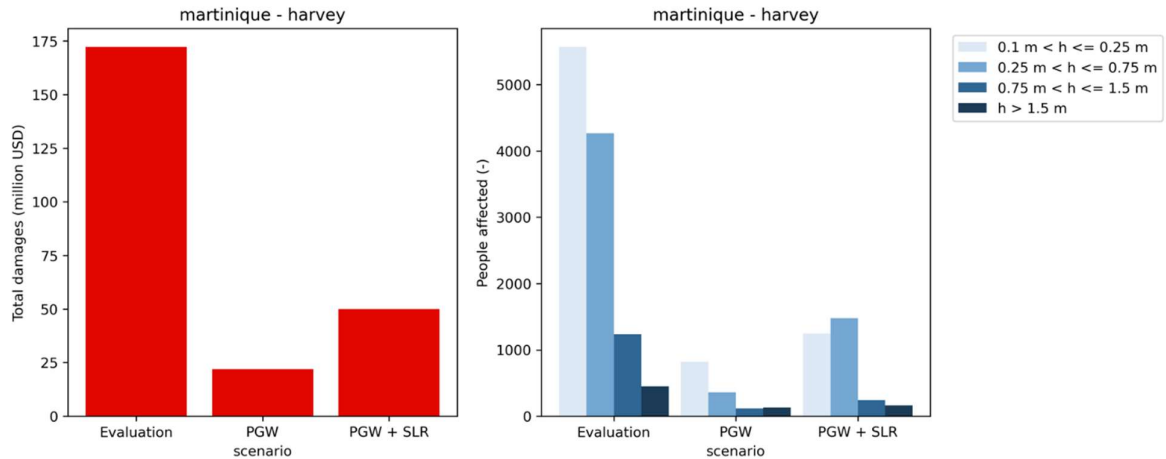


Figure 3.29: Impact indicators for Martinique for 3 scenarios of cyclone Harvey. (Left) Total damages over the whole island for each scenario, (Right) People affected for each scenario and different flood depths, where h is the maximum flood depth during the event

Dominican Republic – Maria

A high percentage of the damages in the evaluation run derive from the flooding of Santo Domingo where most of the population in Dominican Republic is concentrated (Figure 3.30). In the PGW run, damages are ~20% lower (Figure 3.31) which can be attributed to the generally lower flood depths at Santo Domingo (where most of the damages are coming from) due to the track shift. Adding the SLR scenario does not change the total damages estimates for the same reasons.

Additionally, the number of people that are affected by different water depths is calculated using different water depth thresholds. In the evaluation run most people are affected by minor or intense flooding ($0.1 \text{ m} < h < 0.25 \text{ m}$ or $0.25 \text{ m} < h < 0.75 \text{ m}$ respectively), while people that are affected by water major or severe flooding ($0.75 \text{ m} < h < 1.5 \text{ m}$ or $h > 1.5 \text{ m}$ respectively) are around half (Figure 3.31). These numbers are about 10% lower in the PGW (+SLR) runs for the people affected minor or intense flooding, while the decrease is higher (~27%) for the people affected by major or severe flooding.

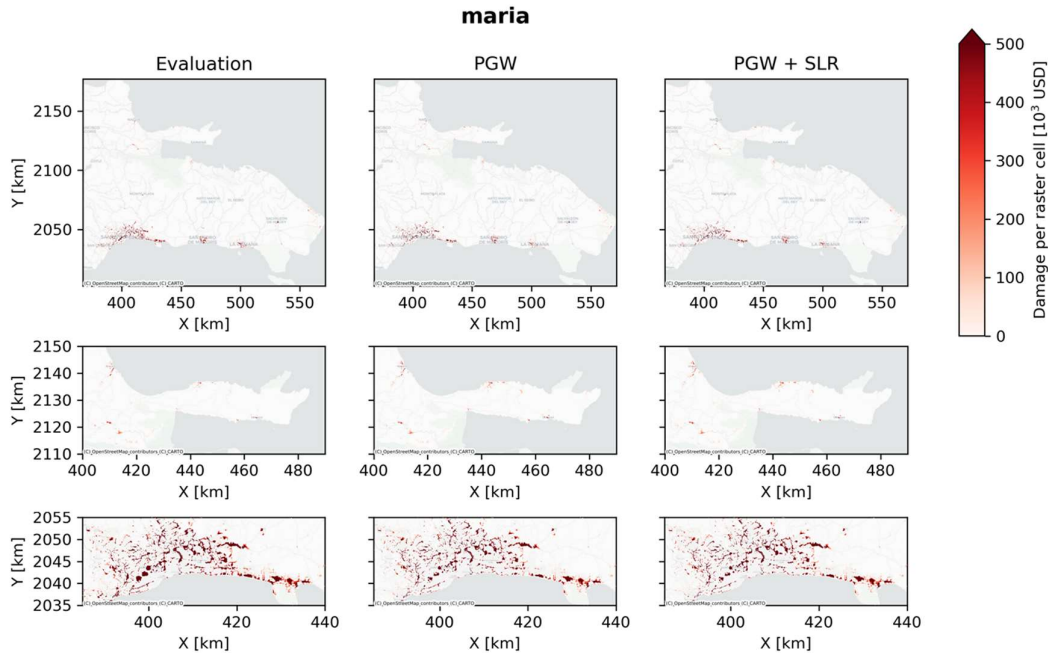


Figure 3.30: Damage maps in USD produced with FIAT for Dominican Republic for 3 scenarios of cyclone Maria. The 3 columns present the 3 different scenarios modelled herein, with the evaluation run, the PGW run and the PGW, including SLR respectively. The top maps include the whole of Dominican Republic, while the bottom maps present 2 zoom-in areas.

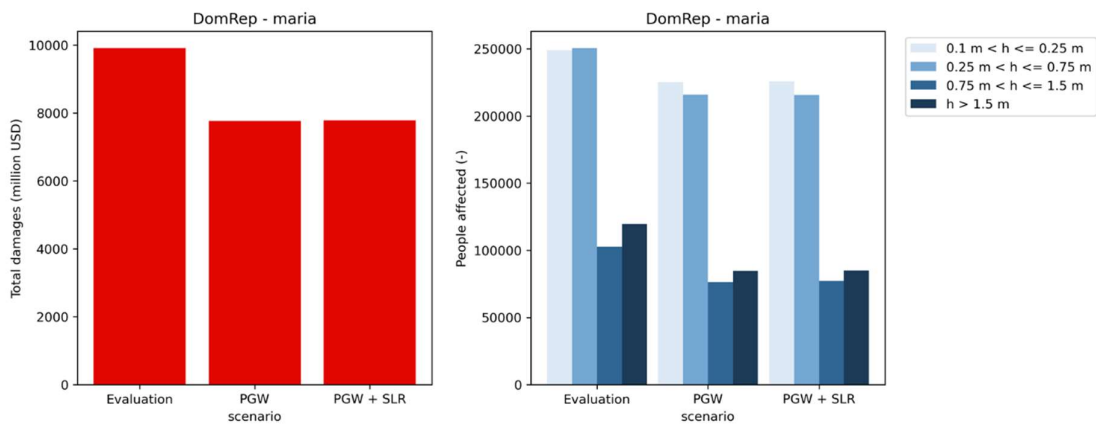


Figure 3.31: Impact indicators for Dominican Republic for 3 scenarios of cyclone Maria. (Left) Total damages over the whole island for each scenario, (Right) People affected for each scenario and different flood depths, where h is the maximum flood depth during the event

St. Martin - Irma

For the evaluation run of cyclone Irma impacts in St. Martin most of the damages modelled with FIAT are concentrated at Marigot (for the French part) and Philipsburg (for the Dutch part) (Figure 3.28). In the PGW run cyclone Jose is considered here since it had a stronger impact on the island. This included higher water levels and precipitation, which resulted in more damages (almost double), covering larger areas (Figure 3.32). With SLR effects added in the PGW run, the damages increase further (by ~30%), since the coastal zones, where much of the exposed population is located, are affected by higher water depths.

As expected, these trends are represented in the people affected indicators as well (Figure 3.33). Around ~30% and ~35% more people are affected by minor and intense flooding respectively in the PGW run, relative to the evaluation run (Figure 3.33). The increase in people affected is quite stronger for the people affected by major and severe flooding reaching values of ~160% and ~270% respectively. Adding the SLR effects, does not change the total number of people affected severely, but an increase in the people affected by higher water depths is observed.

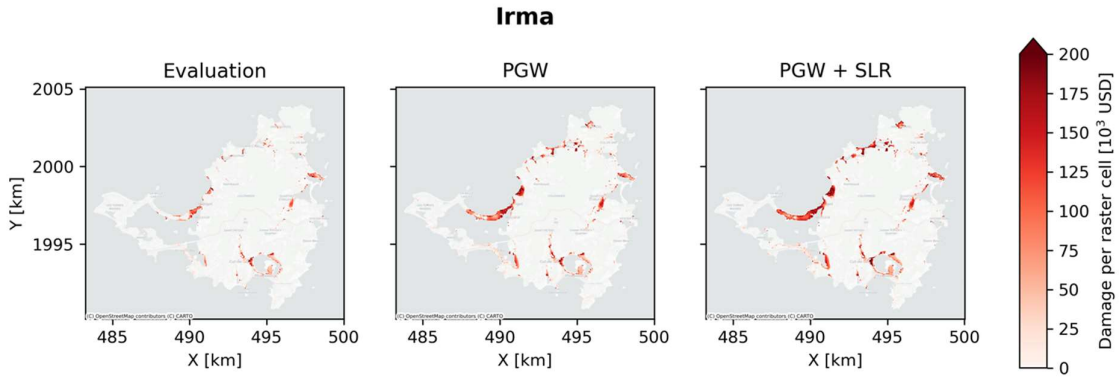


Figure 3.32: Damage maps in USD produced with FIAT for St. Martin for 3 scenarios of cyclone Irma. The 3 columns present the 3 different scenarios modelled herein, with the evaluation run, the PGW run and the PGW, including SLR respectively.

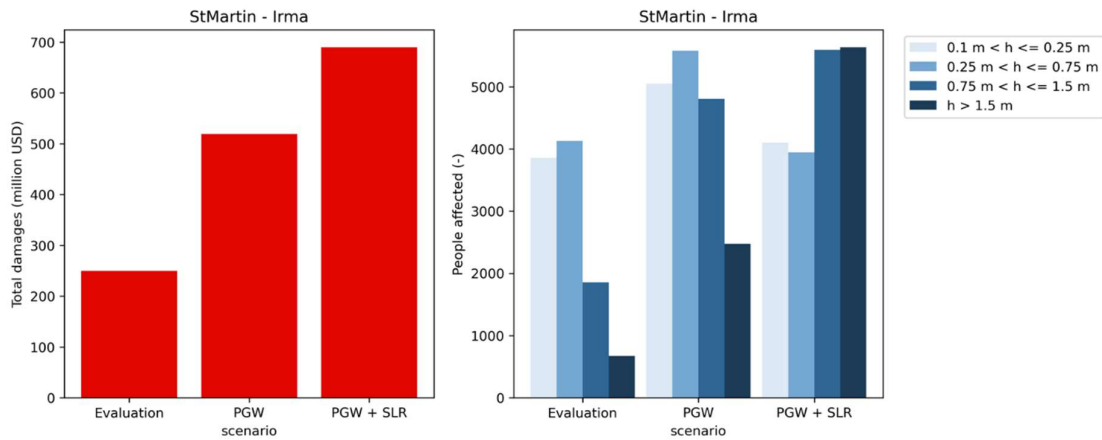


Figure 3.33: Impact indicators for St. Martin for 3 scenarios of cyclone Irma. (Left) Total damages over the whole island for each scenario, (Right) People affected for each scenario and different flood depths, where h is the maximum flood depth during the event

3.1.4 Discussion and lessons learned

To assess future changes in flood impacts caused by tropical cyclones over the Caribbean Islands we implemented a compound flood impact modelling chain for three of these Islands; St. Martin, Martinique and the Dominican Republic. The climate projections that drive the modelling chain were prepared by KNMI using the high-resolution Convection-Permitting Regional Climate Modelling (CP-RCM) system HCLIM in a future pseudo-global warming (PGW) mode. The set of scenarios thus provided consisted of: (1) a historic evaluation run with re-analysis data as boundary conditions, (2) a PGW run, where the boundaries are perturbed with future Delta changes, that provides 'futurized' conditions of the current climate events and (3) a scenario where Sea Level Rise has been added on top of the PGW total sea water levels.

In a first step the meteorological variables, wind speed, air pressure and precipitation were analysed over the full Caribbean modelling domain during the storm periods. In general, the values tend to become more extreme for the PGW scenario compared to the evaluation; higher maximum wind speeds, lower air pressures and higher precipitation intensities and depths.

From these results one could hypothesize that there may as well be an increased flood impact of future tropical cyclones. We investigated this by running the flood impact modelling chain for the three scenarios and analysed the results by looking at the flood impacts of the historic and 'futurized' cyclones. One of the main difficulties of this PGW approach is the large inter-annual variability and the non-linear dynamics of tropical cyclones. This makes a one to one comparison between the evaluation and PGW runs challenging. Already in the evaluation run, the simulated events do not match the observed tracks. As mentioned by the CP-RCM modelers in EUCP Deliverable 3.5: randomly induced track differences may determine the sign of the along-track future changes. For all storms analysed we see changes in position, either moving North (Maria) or South (Jose), as a consequence, we also see changes in strength, wind speed and precipitation intensity overland. We thus obtained future changes in flooding and flood impact that are not primarily caused by climate change, but rather by spatially shifting cyclones.

Only for Irma at Sint-Martin we found clear increases in future floods, but as discussed this may be a result of the observed storms being very close together in the 2017 cyclone season. The future heavy precipitation is caused rather by the intensification of Jose than by the intensification of Irma.

The above complicates the design of the foreseen storyline approach using the PGW simulations. The modelling chain did not provide realistic 'futurized' events. In a future study, instead of directly using the PGW runs to force the hydrological and hydrodynamic models the boundary conditions of the flood modelling chain for the evaluation run could be scaled towards future conditions based on a delta change between the evaluation and PGW scenario. This would be a way to circumvent the change in cyclone track position. Alternatively, large climate model ensembles (van Oldenborgh et al., 2107; Van der Wiel et al., 2019), synthetic event generation (Bloemendaal et al., 2020; Lin et al., 2012) or machine learning approaches could be used to analyse the climate change impact.

In this case-study we explored the value of CP-RCM simulations for understanding flood impacts associated with Tropical Cyclones in the Caribbean using a PGW experiment from one CP-RCM. The multi-model CP-RCM dataset from WP3 would be a valuable instrument to analyse changes in flood patterns in a more statistical founded manor in the future.

3.1.5 Assumptions and simplifications made to complete data requirements

This case-study tested for the first time the value of high-resolution CP-RCM simulations for the assessment of future tropical cyclone flood impact focussing on a single CP-RCM. A number of assumptions and simplifications were necessary in order to apply the CP-RCM simulation to this study, these are listed below together with some recommendations for future improvements.

CP-RCM data and cyclone tracks:

- Due to the high computational challenges the HCLIM data was only available for the storm season (June to October). However, the hydrological model normally runs on continuous time-series and otherwise requires reliable initial states for the storm season. To overcome this problem the initial conditions for the hydrological model were obtained from a continuous run forced with CHIRPS. This was done both for the current and future climate, while in the future moisture conditions may be slightly different due to seasonal climate changes;
- We did not have access to future wave data and thus also used the historic ERA5 wave data for the PGW experiment. This meant that the future wave conditions did not account for future changes in meteorological conditions but were still representing the reanalysis data. Additionally, sometimes the wave time-series had to be shifted a few days in time to ensure they coincided with the future cyclone;
- Most of the Caribbean islands are characterised by a steep topography. This means that storms surge heights are generally small, but that waves are a large driver for extreme sea levels. Unfortunately, significant wave heights were not available from HCLIM simulations. In the absence of information of wave set-up at the coast, we made the commonly used assumption for the wave setup, of 20% of the offshore significant wave height H_s (Vousdoukas et al., 2018) this may have led to under or overestimations of the total wave-induced water setup during the event. A more accurate estimation would require setting up regional models for the estuaries, for which the required data is lacking;
- For Saint-Martin the severe storm Irma is nearly not present in the PGW runs, whether the less severe Jose that followed upon Irma a couple of days later was far more severe in the PGW run. For Saint-Martin we therefore decided to focus on the most severe storm of the cyclone season in the evaluation and PGW experiment instead of the exact same storm. This meant we also had to use the ERA5 waves of Irma for the future simulation of Jose.

Flood impact modelling:

- The accuracy and resolution of global DEMs are a bottleneck in flood hazard studies. Here we opted for the latest available one – FABDEM - which is the COPERNICUS DEM corrected for bias in buildings and forest and has the best available spatial resolution. Still, using local data with higher accuracy and resolution would be needed for more informed decision making at the local scale;
- The same holds for the exposure data (population count and building footprints), for which we had to use global sources, meaning that their local representation might not always be accurate. Additionally, the damages are calculated based on global functions that are based on GDP and simplistic relationships. Therefore, the results should mainly be interpreted based on relative differences rather than absolute values.

3.2 Assessment of future changes in flood and drought extremes for La Reunion

3.2.1 LaReunion - Brief introduction to the case-study

La Reunion is one of the nine European Union (EU) outermost regions (that are geographically very distant from the European continent). La Reunion is an overseas department and region of France. It is an island in the Indian Ocean approximately 550 km (340 mi) east of the island of Madagascar and 175 km (109 mi) southwest of the island of Mauritius (see also Figure 3.34). As of January 2022, it had a population of more than 850000 people³. The island is regularly threatened by tropical cyclones. In 2018, a tropical cyclone caused heavy flooding, while the last devastating cyclone to hit the island came in 2007, killing two people and causing extensive damage. Recently, cyclone Batsirai passed La Reunion⁴. On La Reunion Island drought and warm event intensity is relatively low, however this may change with future climate change. Also changing cyclone storm intensity may impact the island.

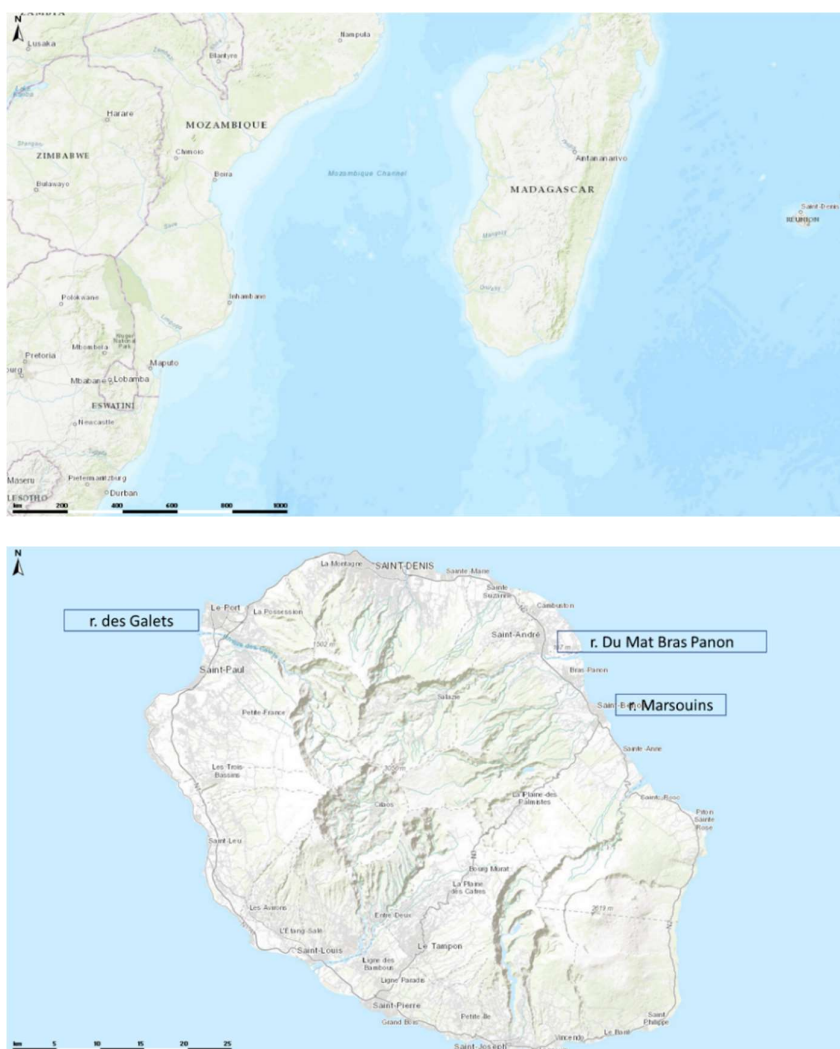


Figure 3.34: Overview of La Reunion (rivers for which discharge data were available and used are indicated).

³ <https://en.wikipedia.org/wiki/R%C3%A9union>

⁴ <https://www.france24.com/en/france/20220203-residents-of-reunion-island-confined-to-homes-as-tropical-cyclone-batsirai-passes-through>

3.2.2 Data and Methods

Observed rainfall & reanalysis

As reference meteorological dataset we used interpolated precipitation fields obtained from MeteoFrance (1979-2019) at 1km² resolution with elevation as external drift. For potential evaporation calculated with De Bruin et al (2016) we used the ERA5 reanalysis. We also checked the use of CHIRPS global rainfall product but this was too coarse and gave poor results compared to the use of the interpolated high resolution rainfall data from MeteoFrance.

CPM simulations CNRM

Runs from CNRM for the current (1990-2010) and future climate (2081-2100) were used to drive a hydrological model for La Reunion. A first check was made to see if a correction on the wet day frequency of rainfall was needed. Figure 3.35 shows that the wet/dry day frequency for the current climate is similar to the observed and therefore no correction (e.g. a threshold) was applied.

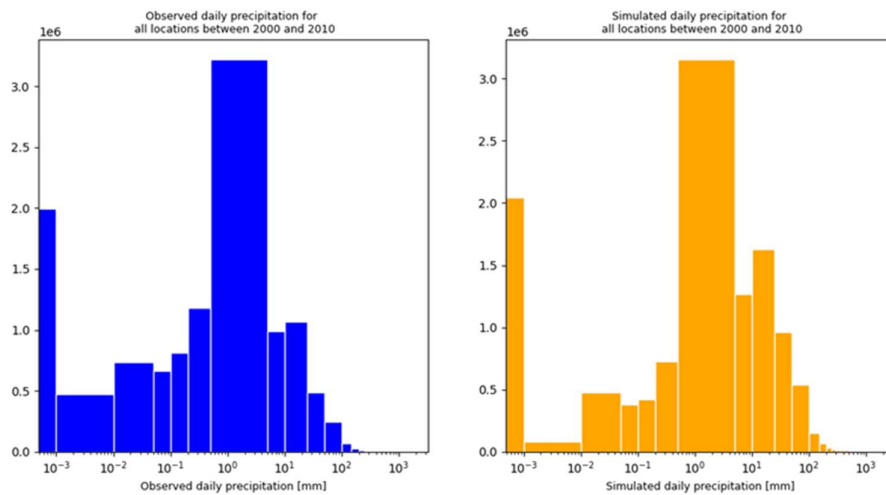


Figure 3.35: Observed and simulated precipitation for the current climate (2000-2010).

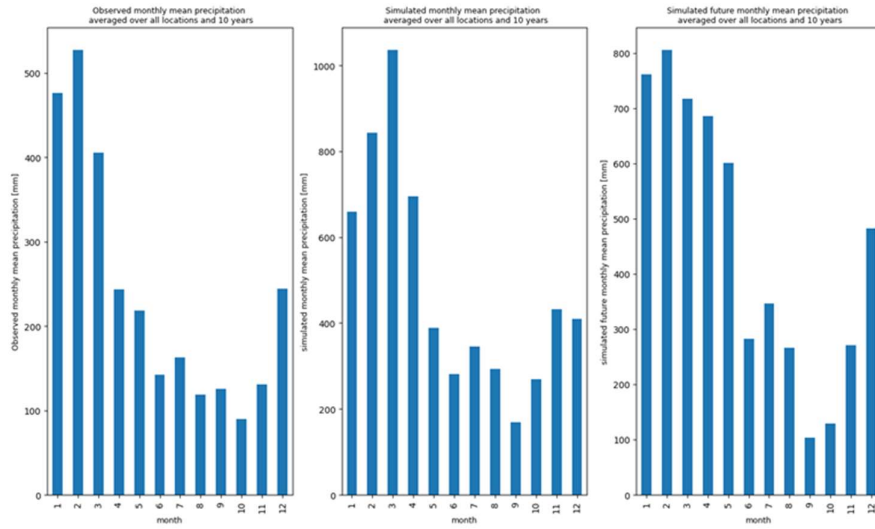


Figure 3.36: Observed and simulated precipitation for current and future climate.

The second step was to check the precipitation depth of the simulations versus observed. Figure 3.36 is showing that the simulated rainfall amount is somewhat too high and therefore it was decided to perform a simple linear scaling bias correction on a monthly basis as shown in Figure 3.37.

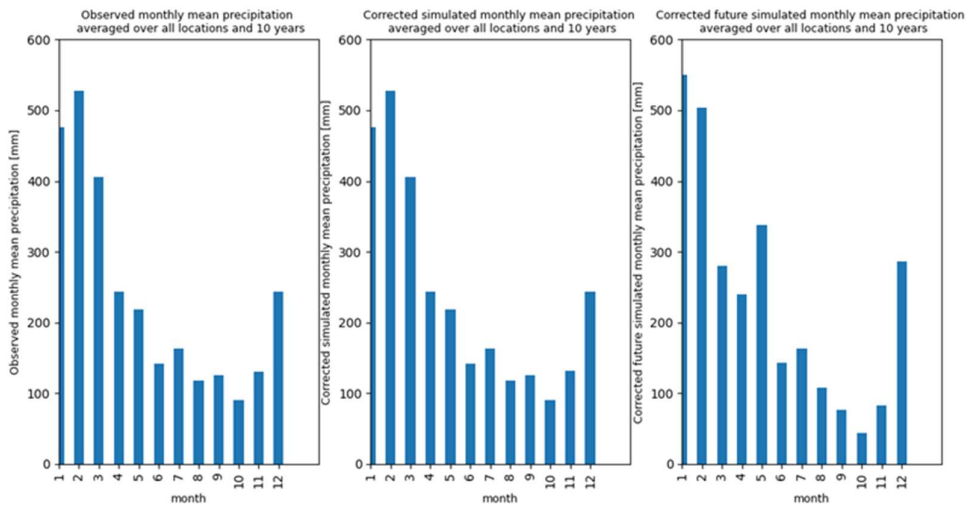


Figure 3.37: Observed and corrected simulated precipitation for current and future climate.

Distributed hydrological model wflow_sbm

Using hydromt (Eilander et al., 2022a), a wflow_sbm model (Imhoff et al. 2020; Eilander et al., 2021) was built at 0.008333 (~1km) and 0.0016333 (~200m) resolution, see example for river network display in Fig. 3.38. The model was forced with both historical data and bias corrected CNRM CPM data (see next paragraph). The model was compared against available discharge observations (available from hydrobanque)⁵. These series were relatively short (10 years) with gaps (sometimes because of cyclones). The model results between the 1km and 200m model were minor and therefore the 1km model is used in the remainder of the report. The same wflow_sbm setup as Imhoff et al (2020) was used for the model parameters, however here we use a ksathorfrac set at 100. This parameter controls the baseflow versus peak flow dynamics.

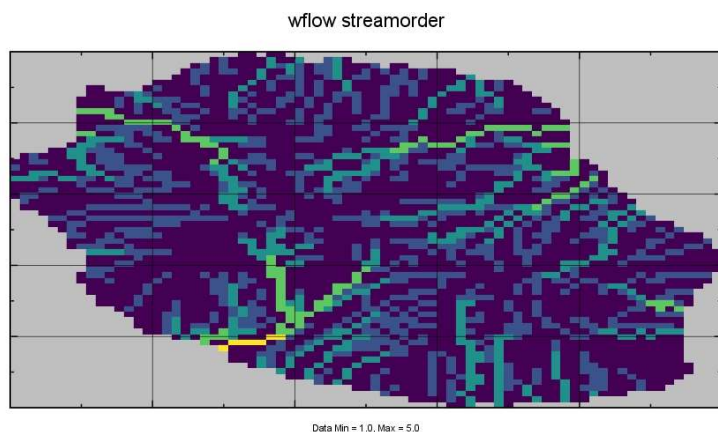


Figure 3.38. derived wflow_sbm streamorder map.

From Fig. 3.39 it can clearly be seen that the simulated extreme discharges are lower than observed. Note however that the uncertainty in both the rainfall and discharges are quite large during extreme events like cyclones. In addition, the rivers may contain several weirs and or reservoirs that impact the discharge measurements. These are small and not yet included in the wflow_sbm model which was setup based on available global data. This may play a role in the low flow simulations of river des Marsouis.

⁵ <https://hubeau.eaufrance.fr>

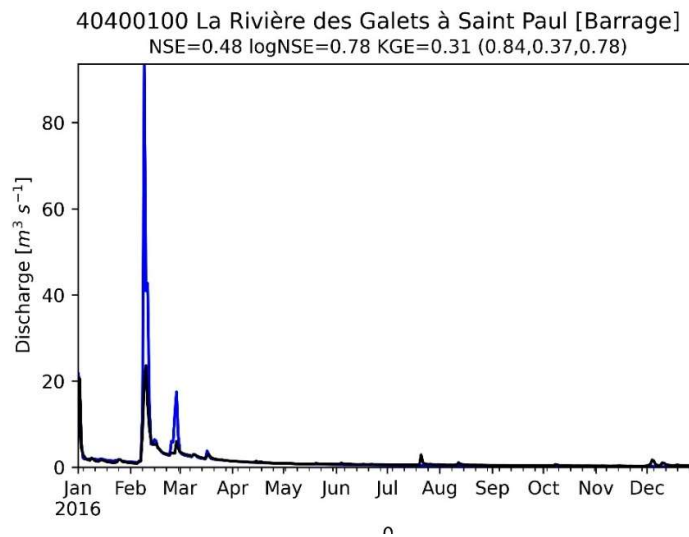
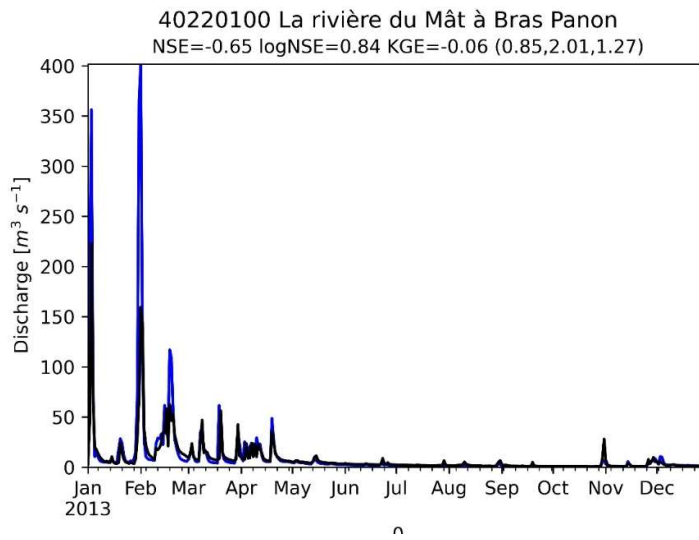
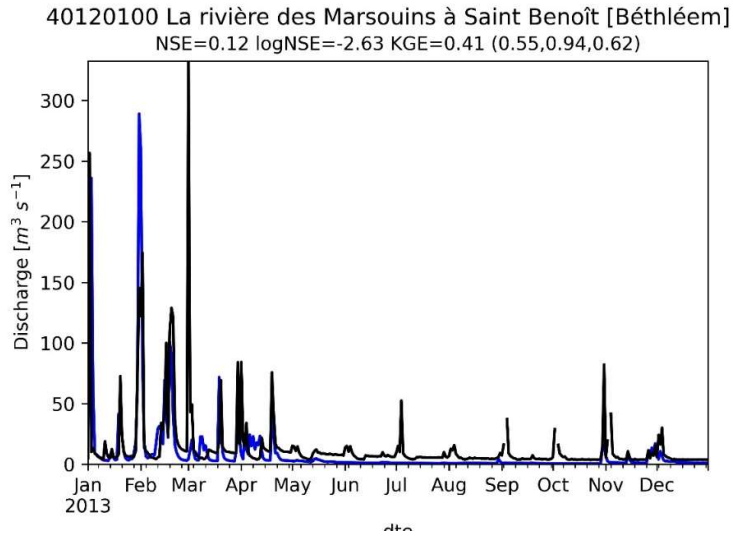


Figure 3.39 Examples of modelled (blue) versus observed (black) discharges for three river gauge locations

3.2.3 Results

Current versus Future climate

The wflow_sbm model was forced with both the bias corrected current and future CPM runs. Most noticeable and in contrast with the flash flooding in the Alps (see deliverable 4.5) where bias correction was not deemed necessary (also not possible because of lack of observational datasets at the right spatial and temporal scale), for La Reunion a bias correction of the CP-RCM data is needed.

The hydrological wflow_sbm model setup was able to mimic observed flows to some degree when forced with local rainfall dataset obtained from MétéoFrance. Note that these small rivers often contain infrastructure to generate power which are not included in this current model. Forcing the model with downscaled CHIRPS or ERA5 rainfall resulted in poor performance (not shown). Also note that the amount (i.e. few years) of validation data (i.e. observed discharges) is rather limited and maybe affected by the operational of hydropower weirs/dams.

Finally, when we look at the delta change of the current and future climate run, we find that the absolute maximum discharge increases 30% with respect to the current climate run. Figure 3.40 shows the most extreme flood years in the two simulations. Note that the years in the title (1996 and 2085) correspond to the simulation years. Figure 3.41 shows the histogram of the yearly maximum discharge also showing an increase in annual maxima. If the actual discharge will increase with 30% is difficult to say. From the comparison with the measurements the flood peaks tend to be overestimated although it also seems that measurement equipment tends to fail under real extreme conditions and the measurement series are relatively short (<10years).

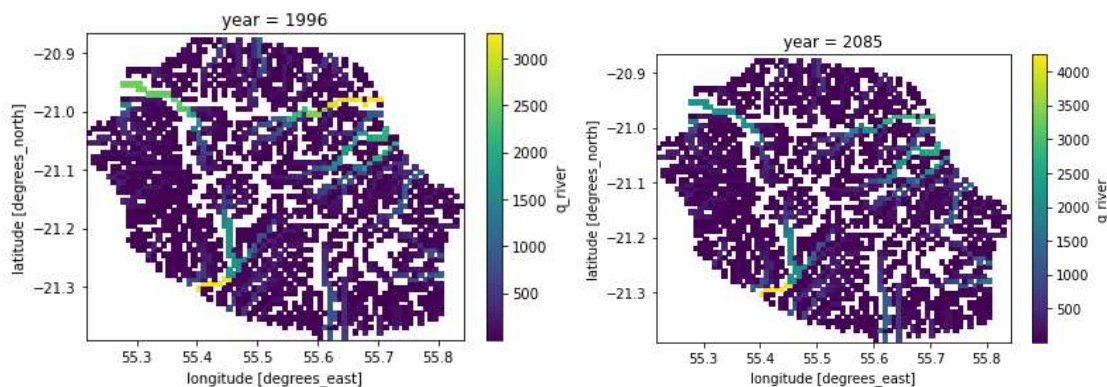


Figure 3.40. Most extreme floods in both current (1996) and future (2085) climate runs showing a ~30% increase for the future.

In contrast the annual mean discharge shows a slight decrease of 2% indicating that the discharge regime will be more variable in the future. This is shown in Figure 3.42.

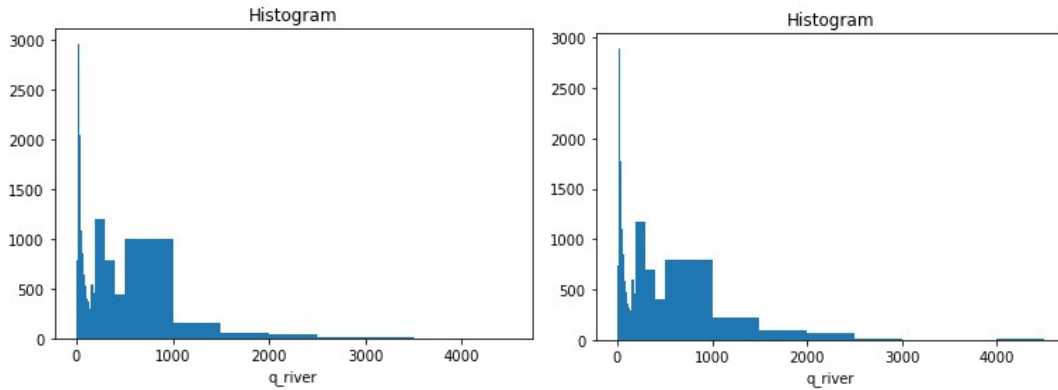


Figure 3.41. Histograms of both current (left) and future (right) climate runs showing an increase in yearly annual maxima for the future.

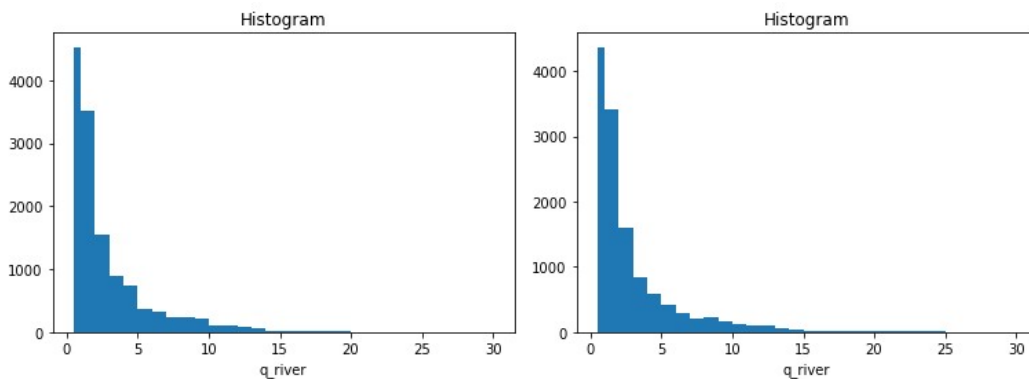


Figure 3.42. Histograms of both current (left) and future (right) climate runs showing a slight decrease in yearly annual mean discharge for the future.

3.2.4 Discussion and lessons learned

A wflow_sbm hydrological model could easily be setup and tested for La Reunion. The wflow_sbm model performs well when driven by local gridded interpolated rainfall forcing. The discharge measurements are relatively short and influenced by reservoirs. These reservoirs are not yet included in the current model setup but can easily be included in future studies.

Compared to other outermost regions the availability of in-situ observations is relatively good for La Reunion.

Bias correction was needed for the CP-RCM runs while it was not deemed necessary for the runs over the Alps.

Based on these simulations, annual extremes in discharge could increase even up to 30% by the end of the century under a high-emissions scenario, potentially causing more devastating flooding across La Reunion.

Based on the simulations, the discharge regime will become more variable as the annual mean discharge decreases slightly (~2%).

References

Andersen, O.B., Knudsen, P., 2009. DNSCO8 mean sea surface and mean dynamic topography models. *J. Geophys. Res. Ocean.* 114. <https://doi.org/10.1029/2008JC005179>

Bates, P.D., Horritt, M.S., Fewtrell, T.J., 2010. A simple inertial formulation of the shallow water equations for efficient two-dimensional flood inundation modelling. *J. Hydrol.* <https://doi.org/10.1016/j.jhydrol.2010.03.027>

Belušić, D., de Vries, H., Dobler, A., Landgren, O., Lind, P., Lindstedt, D., Pedersen, R. A., Sánchez-Perrino, J. C., Toivonen, E., van Ulft, B., Wang, F., Andrae, U., Batrak, Y., Kjellström, E., Lenderink, G., Nikulin, G., Pietikäinen, J.-P., Rodríguez-Camino, E., Samuelsson, P., van Meijgaard, E., and Wu, M.: HCLIM38: a flexible regional climate model applicable for different climate zones from coarse to convection-permitting scales, *Geosci. Model Dev.*, 13, 1311–1333, <https://doi.org/10.5194/gmd-13-1311-2020>, 2020.

Bondarenko, M., Kerr, D., Sorichetta, A., Tatem, A.J.A.A.J., 2020. Census/projection-disaggregated gridded population datasets for 189 countries in 2020 using Built-Settlement Growth Model (BSGM) outputs, WorldPop, University of Southampton, UK.

Buchhorn, M., Lesiv, M., Tsendbazar, N.E., Herold, M., Bertels, L., Smets, B., 2020. Copernicus global land cover layers-collection 2. *Remote Sens.* 12, 1–14. <https://doi.org/10.3390/rs12061044>

Caldwell, P. C., M. A. Merrifield, P. R. Thompson (2015), Sea level measured by tide gauges from global oceans — the Joint Archive for Sea Level holdings (NCEI Accession 0019568), Version 5.5, NOAA National Centers for Environmental Information, Dataset, doi:10.7289/V5V40S7W.

Charnock, H. (1955). Wind stress on a water surface. *Quart. J. Roy. Meteor. Soc.*, 81, 639–640.

De Bruin, H.A.R., Trigo, I.F., Bosveld, F.C. and Meirink, J.F., 2016. A thermodynamically based model for actual evapotranspiration of an extensive grass field close to FAO reference, suitable for remote sensing application. *Journal of Hydrometeorology*, 17(5), pp.1373-1382.

Dullaart, J. C. M., Muis, S., Bloemendaal, N., & Aerts, J. C. J. H. (2020). Advancing global storm surge modelling using the new ERA5 climate reanalysis. *Climate Dynamics*, 54(1–2), 1007–1021. <https://doi.org/10.1007/s00382-019-05044-0>

Eilander, D., van Verseveld, W., Yamazaki, D., Weerts, A., Winsemius, H. C., and Ward, P. J.: A hydrography upscaling method for scale-invariant parametrization of distributed hydrological models, *Hydrol. Earth Syst. Sci.*, 25, 5287–5313, <https://doi.org/10.5194/hess-25-5287-2021>, 2021.

Eilander, Dirk, & Boisgontier, H  l  ne. (2022a). hydroMT (v0.4.5). Zenodo. <https://doi.org/10.5281/zenodo.6107669>

Eilander, D., Boisgontier, H., van Verseveld, W., Bouaziz, L., & Hegnauer, M. (2022b). HydroMT-Wflow: Wflow plugin for HydroMT. <https://doi.org/10.5281/zenodo.6221375>

Eilander, D., Leijnse, T., & Winsemius, H. C. (2022c). HydroMT-SFINCS: SFINCS plugin for HydroMT (Version v0.2.1) [Computer software]. <https://doi.org/10.5281/zenodo.6244556>

Funk, C., Peterson, P., Landsfeld, M. et al. The climate hazards infrared precipitation with stations—a new environmental record for monitoring extremes. *Sci Data* 2, 150066 (2015). <https://doi.org/10.1038/sdata.2015.66>

GEBCO-Compilation-Group, 2021. GEBCO 2021 Grid. <https://doi.org/doi:10.5285/c6612cbe-50b3-0cff-e053-6c86abc09f8f>

HydroMT, 2022. hydroMT: Build and analyze models like a data-wizard!, <https://doi.org/10.5281/zenodo.6107669> (last access 3/24/2022).

Hawker, L., Uhe, P., Paulo, L., Sosa, J., Savage, J., Sampson, C., Neal, J., 2022. A 30 m global map of elevation with forests and buildings removed. *Environ. Res. Lett.* 17, 024016. <https://doi.org/10.1088/1748-9326/ac4d4f>

Hersbach, H, Bell, B, Berrisford, P, et al. The ERA5 global reanalysis. *Q J R Meteorol Soc.* 2020; 146: 1999– 2049. <https://doi.org/10.1002/qj.3803>

Huizinga, J., Moel, H. de and Szewczyk, W. 2017. Global flood depth-damage functions: Methodology and the database with guidelines, JRC Work. Pap. JRC105688, Jt. Res. Cent. (sev. site).

Imhoff, R. O., van Verseveld, W. J., van Osnabrugge, B., & Weerts, A. H. (2020). Scaling Point-Scale (Pedo)transfer Functions to Seamless Large-Domain Parameter Estimates for High-Resolution Distributed Hydrologic Modeling: An Example for the Rhine River. *Water Res. Res.*, 56(4), <https://doi.org/10.1029/2019WR026807>

IPCC, 2021: Summary for Policymakers. In: *Climate Change 2021: The Physical Science Basis. Contribution of Working Group I to the Sixth Assessment Report of the Intergovernmental Panel on Climate Change* [MassonDelmotte, V., P. Zhai, A. Pirani, S.L. Connors, C. Péan, S. Berger, N. Caud, Y. Chen, L. Goldfarb, M.I. Gomis, M. Huang, K. Leitzell, E. Lonnoy, J.B.R. Matthews, T.K. Maycock, T. Waterfield, O. Yelekçi, R. Yu, and B. Zhou (eds.)]. Cambridge University Press. In Press.

Kernkamp, H. W. J., Van Dam, A., Stelling, G. S., & de Goede, E. D. (2011). Efficient scheme for the shallow water equations on unstructured grids with application to the Continental Shelf. *Ocean Dynamics*, 61(8), 1175–1188. <https://doi.org/10.1007/s10236-011-0423-6>

Leijnse, T., van Ormondt, M., Nederhoff, K., van Dongeren, A., 2020. Modeling compound flooding in coastal systems using a computationally efficient reduced-physics solver: including fluvial, pluvial, tidal, wind- and wave-driven processes. *Coast. Eng.* 163, 103796. <https://doi.org/10.1016/j.coastaleng.2020.103796>

Lin, P., Pan, M., Allen, G. H., Frasson, R. P., Zeng, Z., Yamazaki, D., & Wood, E. F. (2020). Global estimates of reach-level bankfull river width leveraging big data geospatial analysis. *Geophysical Research Letters*, 47(7). <https://doi.org/10.1029/2019gl086405>

Lyard, F. H., Allain, D. J., Cancet, M., Carrère, L., & Picot, N. (2021). FES2014 global ocean tide atlas: design and performance. *Ocean Science*, 17(3), 615–649. <https://doi.org/10.5194/os-17-615-2021>

Muis, S., Apecechea Irazoqui, M., Dullaart, J., de Lima Rego, J., Madsen, K. S., Su, J., et al. (2020). A High-Resolution Global Dataset of Extreme Sea Levels, Tides, and Storm Surges, Including Future Projections. *Frontiers in Marine Science*, 7. <https://doi.org/10.3389/fmars.2020.00263>

Muis, S., Verlaan, M., Winsemius, H. C., Aerts, J. C. J. H., & Ward, P. J. (2016). A global reanalysis of storm surges and extreme sea levels. *Nature Communications*, 7(7:11969), 1–11. <https://doi.org/10.1038/ncomms11969>

Neal, J., Hawker, L., Savage, J., Durand, M., Bates, P., & Sampson, C. (2021). Estimating river channel bathymetry in large scale flood inundation models. *Water Resources Research*, 57(5). <https://doi.org/10.1029/2020wr028301>

Nederhoff, K., Hoek, J., Leijnse, T., van Ormondt, M., Caires, S., & Giardino, A. (2021). Simulating synthetic tropical cyclone tracks for statistically reliable wind and pressure estimations. *Natural Hazards and Earth System Sciences*, 21(3), 861–878. <https://nhess.copernicus.org/articles/21/861/2021/>

Pekel, J.F., Cottam, A., Gorelick, N. and A.S. Belward, 2016. High-resolution mapping of global surface water and its long-term changes. *Nature* 540, 418-422 (doi:10.1038/nature20584)

Palacios-Lopez, D., Bachofer, F., Esch, T., Heldens, W., Hirner, A., Marconcini, M., Sorichetta, A., Zeidler, J., Kuenzer, C., Dech, S., Tatem, A.J., Reinartz, P., 2019. New perspectives for mapping global population distribution using world settlement footprint products. *Sustain.* 11. <https://doi.org/10.3390/su11216056>

Schär, C., Frei, C., Lüthi, D. & Davies, H. C. Surrogate climate-change scenarios for regional climate models. *Geophys. Res. Lett.* **23**, 669–672 (1996).

Slager, K., Burzel, A., Bos, E., De Bruikn, K., Wagenaar, D. J., Winsemius, H. C., Bouwer, L. M., and Van der Doef, M. 2016. User Manual Delft-FIAT version 1, available at: <https://publicwiki.deltares.nl/display/DFIAT/Delft-FIAT+Home> (last access: 22 September 2019)

Van der Wiel, K., Wanders, N., Selten, F. M., & Bierkens, M. F. P. (2019). Added value of large ensemble simulations for assessing extreme river discharge in a 2 C warmer world. *Geophysical Research Letters*, 46(4), 2093-2102.

Vousdoukas, M.I., Mentaschi, L., Voukouvalas, E., Verlaan, M., Jevrejeva, S., Jackson, L.P., Feyen, L., 2018. Global probabilistic projections of extreme sea levels show intensification of coastal flood hazard. *Nat. Commun.* 9, 2360. <https://doi.org/10.1038/s41467-018-04692-w>

De Vries et al. (in preparation): Changes in Caribbean hurricanes derived from an ensemble of convection-permitting pseudo-global warming simulation.

Yamazaki D., D. Ikeshima, J. Sosa, P.D. Bates, G.H. Allen, T.M. Pavelsky, 2019. “MERIT Hydro: A high-resolution global hydrography map based on latest topography datasets”. *Water Resources Research*, 2019. DOI: 10.1029/2019WR024873. http://hydro.iis.u-tokyo.ac.jp/~yamadai/MERIT_Hydro/